Accepted Manuscript

Discovery of potent N-(isoxazol-5-yl)amides as HSP90 inhibitors

Danqi Chen, Aijun Shen, Jian Li, Feng Shi, Wuyan Chen, Jing Ren, Hongchun Liu, Yechun Xu, Xin Wang, Xinying Yang, Yiming Sun, Min Yang, Jianhua He, Yueqin Wang, Liping Zhang, Min Huang, Meiyu Geng, Bing Xiong, Jingkang Shen

PII: S0223-5234(14)00884-8

DOI: 10.1016/j.ejmech.2014.09.065

Reference: EJMECH 7372

To appear in: *European Journal of Medicinal Chemistry*

Received Date: 26 August 2014

Revised Date: 19 September 2014

Accepted Date: 19 September 2014

Please cite this article as: D. Chen, A. Shen, J. Li, F. Shi, W. Chen, J. Ren, H. Liu, Y. Xu, X. Wang, X. Yang, Y. Sun, M. Yang, J. He, Y. Wang, L. Zhang, M. Huang, M. Geng, B. Xiong, J. Shen, Discovery of potent N-(isoxazol-5-yl)amides as HSP90 inhibitors, *European Journal of Medicinal Chemistry* (2014), doi: 10.1016/j.ejmech.2014.09.065.

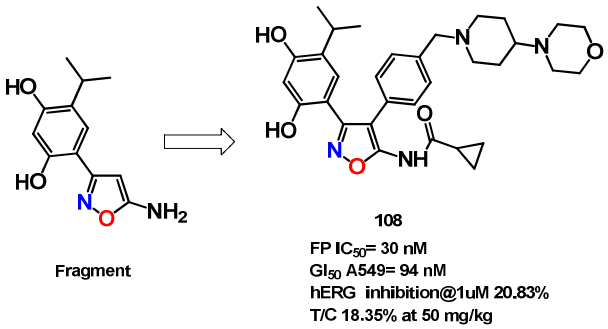

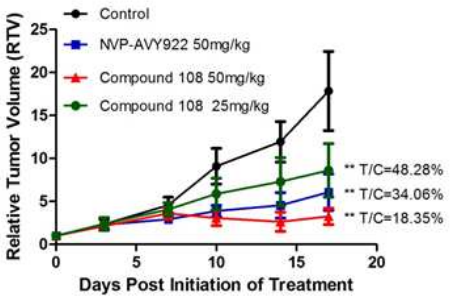

By fragment screening and x-ray crystallography techniques a scaffold of 4,5-diarylisoxazole was selected and developed to a novel series of HSP90 inhibitors with excellent *in vivo* activities.

Discovery of Potent N-(isoxazol-5-yl)amides as HSP90 Inhibitors

Danqi Chen[1#], Aijun Shen[2#], Jian Li[3#], Feng Shi[1], Wuyan Chen[4], Jing Ren[1], Hongchun Liu[2], Yechun Xu[4*], Xin Wang[1] , Xinying Yang[2], Yiming Sun[2], Min Yang[3], Jianhua He[3], Yueqin Wang[2], Liping Zhang[5], Min Huang[2], Meiyu Geng[2*], Bing Xiong[1*], Jingkang Shen[1*]

[1]*Department of Medicinal Chemistry, State Key Laboratory of Drug Research, Shanghai Institute of Materia Medica, Chinese Academy of Sciences, 555 Zuchongzhi Road, Shanghai 201203, China*

[2]*Division of Anti-tumor Pharmacology, State Key Laboratory of Drug Research, Shanghai Institute of Materia Medica, Chinese Academy of Sciences, 555 Zuchongzhi Road, Shanghai 201203, China*

[3]*Shanghai Institute of Applied Physics, Chinese Academy of Sciences, 239 Zhangheng Road, Shanghai 201204, China*

[4]*Drug Discovery and Design Center, Shanghai Institute of Materia Medica, Chinese Academy of Sciences, 555 Zuchongzhi Road, Shanghai 201203, China*

[5]*Department of Pharmacology and Glycobiology, School of Medicine and Pharmacy, Ocean University of China, 5 Yushan Road, Qingdao 266003, People's Republic of China*

[#]*these authors contributed equally*

* Corresponding authors Tel:86-21-50806600-5412 (B.X) E-mail: bxiong@simm.ac.cn; (Y.X) ycxu@simm.ac.cn; (M.G) mygeng@simm.ac.cn; (J.S)jkshen@simm.ac.cn

Abstract

HSP90 is ubiquitously overexpressed in a broad spectrum of human cancers and has been recognized as an attractive target for cancer treatment. Here, we described the fragment screening, synthesis and structure-activity relationship studies of small molecule inhibitors with 4,5-diarylisoxazole scaffold targeting HSP90. Among them, the compound N-(3-(2,4-dihydroxy-5-isopropylphenyl)-4-(4-((4-morpholinopiperidin-1-yl)methyl)phenyl)isoxazol-5-yl)cyclopropanecarboxamide (**108**) showed high affinity for binding to HSP90 (FP binding assay, IC_{50} =0.030μM) and inhibited the proliferation of various human cancer cell lines with

averaging GI_{50} about 88 nM. Compound **108** exhibited its functional inhibition of HSP90 by depleting key signaling pathways and concomitantly elevating of HSP70 and HSP27 in U-87MG cells. Further in vivo studies showed that compound **108** strongly suppressed the tumor growth of human glioblastoma xenograft model U-87MG with T/C =18.35% at 50mg/kg q3w/2.5w. Moreover, compound **108** also exhibited good pharmacokinetic properties. Together, our study implicates that compound **108** is a promising candidate of HSP90 inhibitor and is currently advanced to preclinical study.

Keywords: HSP90; fragment-based drug discovery; crystallography;

Abbreviations list: CDI, 1,1'-Carbonyldiimidazole; DCM, Dichloromethane; DHP, 3,4-Dihydro-2H-pyran; DMAP, 4-Dimethylaminopyridine; DMF, N,N-Dimethylformamide; LHMDS, Lithium Hexamethyldisilazide

1. Introduction

Heat shock proteins (HSPs) comprise a group of evolutionarily conserved proteins divided into five main families on the basis of their molecular weight: HSP110, -90, -70, -60, and the small HSPs. HSPs are required for essential housekeeping functions such as protein folding, assembly, and transportation. HSPs can also redirect damaged and misfolded proteins towards proteasomal degradation and promote cell survival by maintaining the structural and functional integrity of several client proteins that regulate cell proliferation, survival and apoptosis. Among the HSPs, HSP90 is relatively unique because it plays important roles in maintaining the conformation, stability and function of an extensive list of signaling proteins involved in pathways of cell proliferation, cell cycle progression, angiogenesis, invasion and metastasis. Importantly, its client proteins include many key oncogenic proteins, such as Her2, AKT, CDK4, VEGF, MET and ALK, which makes it one of the most attractive antitumor targets [1-6]. It has been well believed that the HSP90 inhibitors can simultaneously affect several abnormal signaling pathways in tumor cells and may also overcome the notorious cancer resistance issue [7-11].

The first identified HSP90 inhibitor Geldanamycin[12], belonging to the macrocyclic polyketide class, was discovered from the bacterial species *Streptomyces hygroscopicus*. Its derivatives 17-AAG and 17-DMAG (Figure 1) were semi-synthesized to improve activity and reduce toxicity

[13-14]. PU3, the first totally synthesized inhibitor of HSP90, was developed with the aid of the structure-based drug design technique [15-16]. Pharmacophore models extracted from PU3 and its derivatives were applied to develop CNF-2024/BIIB021 which entered clinical trials in 2005 [17-18]. Other unique HSP90 inhibitors such as NVP-AUY922 and SNX-5422 were developed by Vernalis and Serenex respectively, and both entered clinical trials in 2007 [19-20]. AT13387, a novel HSP90 inhibitor developed by Astex via fragment-based drug discovery (FBDD) approach is now in phase II clinic trials [21-24]. STA-9090, developed by Synta, has entered phase III clinic trials [25]. However, side effects were commonly observed in HSP90 inhibitors, which limited the clinical studies of these inhibitors. Thus novel structure explorations or modifications are still necessary[26-30].

Figure 1. Reported HSP90 inhibitors

Here we described our work on identification of novel HSP90 inhibitors. Briefly, a focused fragment library was established and screened by direct co-crystallization and X-ray crystallography methods. The structure of N-(isoxazol-5-yl)amides was identified and optimized within structure-based drug design methods to obtain a novel series of HSP90 inhibitors with good pharmacokinetic properties and excellent *in vitro*/*vivo* antitumor activities.

2. Results and Discussion

2.1 Fragment Screening

As demonstrated in previous works from Astex and our group [31], computational docking followed by X-ray crystallography verification is very efficient to identify weak binding fragments in FBDD. In current study, an in-house fragment library containing some commercial available reagents and low molecular weight compounds (about 600 compounds) were docked into the ATP-binding site of N–terminal HSP90. Ten fragments were selected based on the binding interaction patterns. Together with other ten synthesized fragment compounds designed on the basis of known HSP90 inhibitors, totally 20 fragments were subjected to the co-crystallization experiments, and then diffracted with X-ray crystallography techniques to detect their binding. The crystals were diffracted at Shanghai Synchrontron Radiation Facility (SSRF). Among them,

fragment **3** was identified to bind at the ATP site of N-terminus of HSP90. The detailed binding mode was illustrated in Figure **2**.

Figure 2. Binding mode of fragments with HSP90.

Fragment **3** contained a resorcinol group, one of the usually used pharmacophores in HSP90 inhibitors, and an isoxazole group. With detailed analysis of the binding mode of fragment **3**, we found that the N and O of the isoxazole ring and the hydroxyl group on 2'-position of resorcinol interacted with Asp93, Gly97 and Thr184 via the crystal water molecules. The hydroxyl group on 4'-position of resorcinol interacted with Leu48 and Ser52 via another conserved water molecule. The O atom on the isoxazole ring and the amino group at 5-position also formed hydrogen bonds with Gly97 directly. All these interactions formed a network and exhibited a typical binding mode of resorcinol inhibitors of HSP90.

We found that the structure of **3** had a large portion in common with NVP-AUY922 as they both had a resorcinol moiety linking to an isoxazole ring. These two molecules overlapped well at the binding site of HSP90, even the three crystal water molecules (Figure 2B). But as highlighted in Figure 2C and 2D, fragment **3** reversed the O-N position in the isoxazole ring, and had an additional amino group at position 5. The similarity with NVP-AUY922 made fragment **3** a promising hit with predictable good activities while the reversed isoxazole ring might lead some differences from NVP-AUY922. Thus fragment **3** was considered as a good starting point.

2.2 Chemistry

4-Chlororesorcinol and acetic acid took Friedel-Crafts acylation under the catalysis of boron trifluoride to give compound **5**. After benzyl protection of the phenyl hydroxyl groups, compound **6** was transformed via bromoform reaction to acid 7 [19] which was methylated by CH_3I to yield **8**. Under the reaction of LHMDS compound **8** was condensed with anisyl cyanide to give **9**, and followed by cyclization with hydroxylamine hydrochloride to generate **10** [32]. Compound **10** reacted with acryl chlorides and subsequently deprotected by boron trichloride to yield the target compounds **23-35** (Scheme 1).

Scheme 1

As shown in Scheme 2, starting with diverse 5-substituted methyl 2,4-bis(benzyloxy)benzoate, compound **56-60** were synthesized according to the methods described in Scheme 1.

Scheme 2

The hydroxyl groups of 1-(2,4-dihydroxyphenyl)ethanone were protected by benzyl groups to give compound **62** which was submitted to Wittig reaction followed by hydrogenation to generate the isopropyl substituent. Compound **64** took Vilsmeier reaction and then re-protected by benzyl groups to yield **66**. Coupled with hydroxylamine hydrochloride and then chlorinated by N-chlorosuccinimide compound **66** turned to the intermediate **68** [33]. Another intermediate **72** was obtained by hydrolyzation, reduction and dihydropyran protection of commercial available 4-cyanomethylbenzoic acid methyl ester. Compound **68** and **72** were coupled to generate isoxazole **73** which was amidated and deprotected to give **75**. The hydroxyl group was activated by methanesulfonyl chloride, substituted with different amines and then debenzylation to yield the target compounds **93-108**.

Scheme 3

2.3 Structure-Activity Relationships and Structural Studies

Fragment **3** was too small to show strong inhibition. Referring to previous SAR studies on NVP-AUY922 [19], a methoxyphenyl group was introduced to 4-position on the isoxazole ring of fragment **3**. Considering synthetic difficulties, the isopropyl group was replaced by a chlorine atom at this initial optimization stage and the dissociative amino group of 5-position was derivatized to amide to obtain compound **24**. This compound showed an IC_{50} of 0.070 μM in HSP90 fluorescence polarization (FP) assay (Table 1). Further cellular assay showed that it effectively inhibited the growth of A549 cancer cell line with GI_{50} about 7.198 μM.

The crystal structure of the complex of compound **24** with HSP90 was solved and illustrated in Figure **3**. The resorcinol moiety and the isoxazole ring of compound **24** had the same binding

mode with fragment **3**. The incorporated p-methoxyphenyl group also fitted well within the binding site of the protein. These results made compound **24** a promising lead for further SAR study.

Figure 3. Crystal structure of Compound **24** bound to N-terminal HSP90 (PDB ID: 4LWE).

The initial optimization was focused on 5-position of the isoxazole ring. Amides with diverse chains and rings were synthesized. As shown in Table 1, when R_1 was small chains such like Me-, Et-, Pr- , Bu-, or cycloaliphatic rings from cyclopropyl to cyclohexyl, most of the compounds retained the binding affinities (<0.1 μM) on molecular level; when a longer chain was selected for R1 such as **34**, the inhibition activity decreased considerably. However, these compounds showed large differences in cellular assay. The activities ranged from less than 1.0 μM to over 40 μM. Among these compounds, **30** with a cyclopropane carbonyl group was the most potent one with GI_{50} 0.761 μM on A549 cell. Compound **35** with a carbamide structure showed no advantage over the amides in the enzymatic FP assay and was no longer concerned.

Table 1. Binding (FP Assay) and Cell Growth Inhibition (SRB Assay) Data of **23-35**

From the co-crystal structure of compound **24** with HSP90, it was found that the subsite accommodating chlorine at the 5'-position of the resorcinol had more space for optimization. During the following modifications focused on R_2, methyl and isopropyl group were selected for R_1 considering the availability of raw materials. As shown in Table 2, most of the compounds retained the binding affinities. The compounds with R_2 substituted by H (**57**) or a relatively big group (tert-butyl, **59**) showed decreased inhibition activities, especially in the cellular assay. Among these compounds, **60** was found to have most potent cellular activity. Together with the enzymatic binding activity of compound **30**, it indicated that the structure with c-Pr at R_1 and i-Pr at R_2 could benefit the cellular permeability. Therefore, these groups were fixed in later optimization.

Table 2. Binding (FP Assay) and Cell Growth Inhibition (SRB Assay) Data of **56-60**

To check the binding of **60** with HSP90, the co-crystal structure was solved at 1.7Å resolution. The resorcinol moiety and the isoxazole ring bind to the same subsite in HSP90, and the methoxyphenyl group points toward the solvent range (Figure 4A). Therefore, a number of hydrophilic pieces were used to modify the methoxyphenyl group of compound **60** intending to increase the solubility as well as to tune the properties of drug-likeness. As shown in Table 3, the incorporation of hydrophilic groups did not affect molecular activities. Most of them exhibited FP IC_{50} better than 0.05 μM, which confirmed that R_3 was a suitable part for pharmacokinetic optimization. Most of the compounds also showed excellent inhibition activities on cellular level, among which compounds **93**, **102**, and **108** exhibited the GI_{50} less than 0.1 μM. We also solved the co-crystal structure of **93** with HSP90 to verify the binding mode. As illustrated in Figure 4B, the morpholine ring stretches to the solvent as expected. Based on the cellular activities, compounds **93**, **102** and **108** were selected for further investigation.

Figure 4. A. Complex of compound **60** with HSP90 (PDB ID: 4LWI); B. Complex of compound **93** with HSP90 (PDB ID: 4LWH).

Table 3. Binding (FP Assay) and Cell Growth Inhibition (SRB Assay) Data of **93-108**

2.4 Cancer Cell Lines Panel Test

A panel of 15 human cancer cell lines from diverse tissue origins including lung, liver, colon, breast, ovary, prostate, kidney, cervix and skin were selected to evaluate the antitumor efficacy of compounds **93**, **102** and **108** using SRB assay. All these three compounds displayed potent cytotoxicity with average GI_{50} at 0.057, 0.058 and 0.088 μM respectively, indicating their broad-spectrum antitumor activities (Table 4).

Table 4. Cell Growth Inhibition of Compounds **93**, **102** and **108** in Various Human Cancer Cell

2.5 hERG Safety Assay.

Blockade of hERG K+ channels is one of the most important molecular mechanisms of cardiac

arrhythmia, which is a common cause of the failures of many antitumor drugs. Therefore, inhibitory liability on hERG (causing QT prolongation) has become a major safety concern during the development of therapeutic drugs. Compounds **93**, **102** and **108** were subjected to hERG safety assay. As shown in Table 5, compound **102** revealed higher probability of hERG toxicity than compounds **93** and **108**, therefore was filtered out for further study.

Table 5. HERG safety assay of compounds **93**, **102** and **108**.

2.6 Effects on Client Proteins *In vitro*

Human glioblastoma cell line U-87 MG which had been reported to be highly sensitive to NVP-AUY922 was selected to evaluate the ability of compounds **93** and **108** of inhibiting Hsp90 in cancer cells. U-87 MG cells were exposed to increased concentrations of compounds **93** and **108** for 24 h, after that the expression and/or phosphorylation of various client proteins and heat shock proteins were determined by western blotting. As shown in Figure 5, molecular co-chaperone HSP70 and HSP27 were induced effectively, indicating that these compounds inhibited HSP90 directly. Accordingly, the expression level of c-Met and its downstream signaling, namely the phosphorylation of Akt and Erk, were reduced at concentration of 50 nmol/L and barely detectable at 100 nmol/L. All these results were re-obtained by NVP-AUY922 which was taken as a positive control. Collectively, these data supported directly that the effects of compounds **93** and **108** on cell proliferation were a consequence of functional inhibition of HSP90.

Figure 5. Western Blotting analysis of the expression of co-chaperone and client proteins of HSP90 after incubation with compounds 93 and 108 in U-87 MG cells.

2.7 *In vitro* Metabolic Stability. Compounds **93** and **108** were tested on rat and human liver microsome (RLM and HLM, respectively) tissues to evaluate their *in vitro* metabolic stability (Table 6). When the value of RLM and HLM is below 100 μL/min/mg protein, the compound is considered to be metabolically stable. As shown in Table 6, compounds **93** and **108** both showed relatively good stability, especially compound **108**. Both compounds had direct inhibition (>50%)

on CYP2D6 at 10 μM concentration. Compound **93** also had obvious inhibition (>50%)) on CYP2C9. Neither of them showed high inhibition (>200 10^{-4}/min) on CYPs in time-dependent inhibition (TDI) tests. In these tests the results of compounds **93** and **108** were equivalent or slightly better than NVP-AUY922.

Table 6. Metabolic stability and inhibition of rat and human liver microsomes by compounds **93**, and **108**.

2.8 Pharmacokinetic (PK) Profiles. Pharmacokinetic parameters of compounds **93** and **108** in mice after i.v. and p.o. dosing were summarized in Table 7. Comparing the parameters of **93** and **108**, it was found that compound **108** had longer half-life (6.46 hours) and higher AUC value over **93** with iv injection. Therefore compound **108** was advanced to *in vivo* antitumor study.

Table 7. Pharmacokinetic profiles of compounds **93** and **108.**

2.9 *In vivo* Antitumor Study

According to former results, finally, compound **108** was selected to evaluate its *in vivo* anti-tumor activity using mice bearing U-87 MG xenograft tumors whereas NVP-AUY922 was chosen as a reference compound. Compound **108** in form of hydrochloride salt was intravenously injected at doses of 25 and 50 mg/kg 3 times per week for 17 consecutive days. As shown in Figure 6, compound **108** showed statistically significant tumor growth inhibition. The T/C values of compound **108** were 48.28% at 25 mg/kg and 18.35% at 50 mg/kg, which was obviously better than NVP-AUY922 (T/C values was 34.06% at 50 mg/kg). Compound **108** was also well tolerated, exhibiting no serious treatment-related toxicity at these doses and minimal weight loss over the course of this study.

Figure 6. *In vivo* anti-tumor effect of compound 108 in U-87 MG xenograft model.

3. Conclusions

Obtained from fragment screening and with the aids of X-ray crystallography techniques,

fragment **3** was developed to a novel series of HSP90 inhibitors. Compound **108**, one in this series, exhibited strong inhibition of HSP90 in both molecular and cellular level. It also showed good results in pharmacokinetic and safety experiments, which were not less than the reference compound NVP-AUY922. Furthermore the compound significantly inhibits the tumor growth in xenograft cancer model U-87 MG, almost twice strong than NVP-AUY922. These indicated that although compound **108** had a part in common with NVP-AUY922 the reversed isoxazole ring and different side chains did make contribution to the activities. The overall properties warrant compound **108** a promising candidate of Hsp90 inhibitor and this compound is now under further evaluation.

4. Experiment and Methods

4.1 HSP90 expression and purification

The sequence-verified cDNA(NCBI reference sequence: NM_005348.3) encoding the human full-length Hsp90α protein was inserted into the pFastBac-HTb plasmid(Invitrogen, USA). Recombinant bacmid was generated by transposition in *E.Coli*, and transfected into SF9 insert cells using Cellfectin II reagent (Cat no. 10362100, Invitrogen, USA). Large-scale protein production was performed in SF9 insert cell cultures infected with high-titer Hsp90α recombinant baculovirus. Cells were harvested by centrifugation after 96h post infection and stored at -80 ^{o}C until use. The cell pellet was resuspended in lysis buffer (50 mM Tris, pH 7.5, 500 mM NaCl, 10% glycerol and 20 mM imidazole). And protein was eluted with the same buffer containing 250 mM imidazole and concentrated to 1mg/ml. Protein preparations were divided to small aliquots, flash frozen in liquid nitrogen, and stored at -70 ^{o}C.

4.2 FP Enzymatic assay

Based on a test set of Hsp90α inhibitors competing with fluorescent geldanamycin(GM-BODIPY) for binding to Hsp90α, the assays were performed on a multi-mode microplate reader (Synergy4, Bio-Tek, Company, USA). All experiments were conducted in 384-well black flat-bottomed polystyrene plates (Corning no. CLS3575) in a total volume of 40uL for each well. All inhibitors and GM-BODIPY were prepared in DMSO and diluted with the assay buffer (20mM Hepes, pH7.3, 50mM KCl, 5mM $MgCl_2$, 20mM Na_2MoO_4, 0.01% NP40, 0.1mg/ml BSA and 2mM DTT). For each assay, background wells (buffer only), negative controls (GM-BODIPY only) and

positive controls (GM-BODIPY in the presence of Hsp90α) and test wells (inhibitors and GM-BODIPY in the presence of Hsp90α) were included on each assay plate. And the assay plate was incubated at 4 ^{o}C for 16h. The FP values were measured at room temperature with excitation wavelength at 485 nm and emission wavelength at 535 nm. All experimental data were analyzed using the Origin 7.5 software (OriginLab, USA).

4.3 HSP90 (residues 9–236) expression, purification and crystallography

4.3.1 Protein purification and crystallization

A cDNA fragment encoding the N-terminal domain of human Hsp90 (residues 9–236), Hsp90N, was cloned into a pET28 vector. The recombinant plasmid pET28-Hsp90N was transferred into E. coli strain BL21 (DE3) for overexpression (Invitrogen, Carlsbad, USA). Bacterial cultures were grown in LB medium at 37 ℃ to an OD600 of 0.6 – 0.8, and 0.2 mM isopropyl-b-D-thiogalactopyranoside was then added for further growth at 30 ℃ for another 5 h. The harvested cells were re-suspended in lysis buffer (20 mM Tris/300 mM NaCl/5 mM b-mercaptoethanol/10% glycerol, pH 7.5) and sonicated. The resulted suspension was centrifuged and the supernatant was passed through a nickel-bead column (GE Healthcare, Piscataway, USA). The column was then washed with 20 mM imidazole/ 300 mM NaCl/20 mM Tris/5 mM b-mercaptoethanol/10% glycerol, pH 7.5 (wash buffer), until no further protein was eluted. The recombinant Hsp90N was then eluted with 100 mM imidazole/300 mM NaCl/20 mM Tris/5 mM b-mercaptoethanol/10% glycerol, pH 7.5 (elution buffer). The eluted proteins were concentrated (Millipore, Billerica, USA) and then injected into a 120 ml Hiload Superdex75 column (GE Healthcare) from which Hsp90N was eluted with 20 mM Tris/300 mM NaCl/5 mM b-mercaptoethanol/ 10% glycerol, pH 7.5. The fractions containing Hsp90N were collected and concentrated to 20 mg/ml for crystallization. The purity of protein was assessed by SDS-PAGE to be 95%.

Crystals of the Hap90N-RL1 complex (PDB code: 4L8Z) was obtained by the hanging drop vapor-diffusion method in a 24-well plate. RL1 was added in portions to a final concentration of 2 mM, to a protein solution (20 mg/mL). Then 1 μL of the protein−ligand solution was mixed with 1 μL of reservoir solution consisting of 20%–25% (w/v) PEG 2000 monomethyl ether/200 mM magnesium chloride/100 mM sodium cacodylate, pH 6.5. The plate was incubated at 4 ℃, and crystals appeared within 3-5 days. The crystals were quickly transferred to a cryosolution consisting of 25% (w/v) PEG 2000 monomethyl ether/200 mM magnesium chloride/100 mM sodium cacodylate, pH 6.5, 25% (v/v) glycerol, and then flash frozen in liquid nitrogen. Crystals of the Hsp90N-S29 complex (PDB code: 4L91) and the Hsp90N-S46 complex (PDB code: 4L94) were obtained by the hanging-drop vapor-diffusion method in a 24-well plate. Compounds were

added incrementally to a final concentration of 2 mM, to a protein solution (20 mg/mL). 1 μL of the resulting protein−ligand solution was mixed with 2 μL of reservoir solution consisting of 20%–25% PEG4000/ 200 mM magnesium chloride/100 mM Tris at pH 8.5. The plate was incubated at 4 ℃, and crystals appeared within 2-7 days. The crystals were quickly transferred to a cryosolution consisting of 25% PEG4000/ 200 mM magnesium chloride/100 mM Tris at pH 8.5, 25% (v/v) glycerol and then flash frozen in liquid nitrogen.

4.3.2 Data collection, structure determination, and refinement

Crystals were grown and then mounted and flash-frozen in liquid nitrogen for diffraction test and data collection. All data sets were collected at 100 K on beamline BL17U1 at the Shanghai Synchrotron Radiation Facility (SSRF, Shanghai, China) and were processed with the HKL2000 software package. The structures were solved by molecular replacement, using the PHENIX. The search model used for the crystals of apo was the previously reported structure of the Hsp90-ATP (PDB code 3T0Z), the structures were refined using PHENIX. With the aid of the program Coot, compounds, water molecules, and others were fitted into to the initial Fo–Fc map.

4.4 Cell Proliferation Assay

Cells were seeded in 96-well culture plates. On the next day, cells were exposed to various concentrations of compounds and further cultured for 72 h. Finally, cell proliferation was determined using sulforhodamine B26 methods. The inhibition rate was calculated as (1-A515 treated/A515 control) ×100%. The cytotoxicity of compounds was expressed as an IC_{50}, determined by the Logit method.

4.5 Western Blot Analysis. U-87 MG cells were cultured under regular growth conditions to exponential growth phase. Then the cells were treated with the indicated concentration of compounds for 24 h at 37 ℃ and lysed in 1 × SDS sample buffer. Those cell lysates were subsequently resolved on 10% SDS-PAGE, and transferred to nitrocellulose membranes. The blots were incubated with specific primary antibodies, then subsequently with anti-rabbit or anti-mouse IgG horseradish peroxidase. Immunoreactive proteins were detected using an enhanced chemiluminescence detection reagent.

4.6 Pharmacokinetic study

Microsomes (Human microsome: Xenotech, Lot No.H0610; Rat microsome: Xenotech, Lot No. R1000) (0.5 mg/mL) were pre-incubated with 1 μM test compound for 5 min at 37 ℃ in 0.1 M

phosphate buffer (pH 7.4) with 1mM EDTA, and 5 mM $MgCl_2$. The reactions were initiated by adding pre-warmed cofactors (1 mM NADPH). After 0, 5, 10, and 30min incubations at 37 ℃, the reactions were stopped by adding an equal volume of cold acetonitrile. The samples were vortexed for 10 min and then centrifuged at 10,000 g for 10 min. Supernatants were analyzed by LC/MS/MS for the amount of parent compound remaining, and the corresponding loss of parent compound also determined by LC/MS/MS.

The five CYP (CYP3A4, CYP2D6, CYP2C9, CYP1A2 and CYP1C19) enzymatic activities were characterized based on their probe reactions. Incubation mixtures were prepared in a total volume of 100 μl as follows: 0.2 mg/mL microsome (Human microsome: Xenotech, Lot No.H0610), NADPH (1 mM), 100 mM phosphate buffer (pH 7.4), probe substrates cocktail (midazolam 10 μM, testosterone 100 μM, dextromethorphan 10 μM, diclofenac 20 μM, phenacetin 100 μM and mephenytoin 100 μM) and 10 μM tested compound or positive control cocktail（ketoconazole 10 μM，quinidine 10 μM，sulfaphenazole 100 μM, α-naphthoflavone 10 μM, tranylcypromine 1000 μM or negative control (PBS). The final concentration of organic reagent in incubation mixtures was less than 1% v/v. There was a 5 min pre-incubation period at 37 ^{o}C before the reaction was initiated by adding a NADPH-generating system. Reactions were conducted for 20 min for CYP3A4, CYP2D6 and CYP1A2. For each probe drug, the percentage of metabolite conversion was less than 20% of substrate added. The inhibition rate was calculated as: (The formation of the metabolite of probe substrates with 10 μM tested compound) / (The formation of the metabolite of probe substrates with PBS) × 100%.

4.7 *In vivo* U-87 MG Xenograft model study

Animal experiments were performed according to institutional ethical guidelines of animal care. Xenograft U-87 MG was tumor cell lines derived. Well-developed tumors were cut into 1-mm3 fragments and transplanted s.c. into the right flank of nude mice using a trocar. When the tumor volume reached 100 to 150 mm^3, the mice were randomly assigned into control and treatment groups. Control groups were given vehicle alone, and treatment groups received compounds as indicated doses via intravenous injection 3 days per week for 17days. The sizes of the tumors were measured twice per week using microcaliper. The tumor volume (TV) was calculated as: TV = (length × width2)/2, and the relative tumor volume (RTV) was calculated as: $RTV = V_t/V_0$, where V_t is the tumor volume on the day measured and V_0 is the tumor volume on the first day of

treatment. Relative tumor volume was shown on indicated days as the median relative tumor volume ± SE indicated for groups of mice. T/C values were calculated on the final day of study for drug-treated compared with vehicle-treated mice as ($RTV_{Treated}/RTV_{Control}$)×100%.

4.8 Chemistry

General: Reagents (chemicals) were purchased from Alfa-Aesar (Karlsruhe, Germany), Acros (Geel, Belgium), Aldrich (St. Louis, MO, USA), Adamas-beta (Shanghai, China) and Shanghai Chemical Reagent Company (Shanghai, China) and were used without further purification. Analytical thin-layer chromatography was performed on HSGF 254 (150–200 mm thickness; Yantai Huiyou Company, Yantai, Shandong, China). 1H NMR (300 MHz or 400 MHz) spectra were recorded on a Varian Mercury-300 or 400 High Performance Digital FT-NMR with TMS as an inter-nal standard. HPLC analysis was performed using a Gilson HPLC system with UV detection at 214 and 254 nm. LC–MS spectra were obtained on an LCQ Deca XP ion trap mass spectrometer (Thermo-Finnigan, San Jose, CA, USA). Accurate mass measurements were carried out on a Q-TOF ultima Globe mass spectrometer (Micromass, Manchester, UK).

1-(5-Chloro-2,4-dihydroxyphenyl)ethanone (5). 4-Chlororesorcinol (61 g, 0.42 mol) was suspended in boron trifluoride etherate (290 mL) and added acetic acid (25.1 mL, 0.42 mol) dropwise under argon protection. The mixture was heated to 90 ^{o}C for 3.5h. Yellow precipitation formed when the mixture cooled down to room temperature. The mixture was poured into 1 L 10% (w/v) sodium acetate solution and stirred vigorously for 2.5 hours. The yellow precipitate was filtered, washed with water and dried overnight to yield the title compound **5** (67 g, 85%): ^{1}H NMR (300 MHz, DMSO-d_6) δ 12.35 (s, 1H), 11.45 (s, 1H), 8.03 (s, 1H), 6.62 (s, 1H), 2.70 (s, 3H); MS (EI): 186 $[M]^{+}$.

1-(2,4-Bis(benzyloxy)-5-chlorophenyl)ethanone (6). Compound **5** (67 g, 0.36 mol) and potassium carbonate (124 g, 0.9 mol) were suspended in acetonitrile (600 mL) and added benzyl bromide (100.5 mL, 0.84 mol) dropwise. The mixture was refluxed overnight and cooled to room temperature. Most of the solvents were removed in vacuo, and the residue was added 1 L water. White solid formed when the mixture was stirred at room temperature. The solid was filtered, washed with water and petroleum subsequently, and dried to obtained the title compound as white solid (123.6 g, 94%): ^{1}H NMR (300 MHz, $CDCl_3$) δ 7.91 (s, 1H), 7.42-7.32 (m, 10H), 6.55 (s, 1H), 5.13 (s, 2H), 5.07 (s, 2H), 2.54 (s, 3H); MS (EI): 366$[M]^{+}$.

2,4-Bis(benzyloxy)-5-chlorobenzoic acid (7). Compound **6** (1.1 g, 3 mmol) was suspended in sodium hydroxide solution (1.2 g, 30 mmol in 10 mL water) and dioxane (10 mL) and added bromine (1.44 g, 9 mmol) dropwise. The mixture was stirred at ambient temperature overnight. Most of the dioxane was removed in vacuo. 2M HCl was added to the residue to make the pH to 2. Pale-yellow solid formed. The solid was filtered, washed with water, and dried to obtained the title compound (0.9 g, 81%): ^{1}H NMR (300 MHz, $CDCl_3$) δ 10.50 (br, 1H), 8.20 (s, 1H), 7.45-7.35 (m, 10H), 6.64 (s, 1H), 5.20 (d, 4H); MS (EI): 368$[M]^+$.

Methyl 2,4-bis(benzyloxy)-5-chlorobenzoate (8). Compound **7** (1 g, 2.7 mmol) and potassium carbonate (1 g, 7 mmol) were suspended in acetonitrile (50 mL) and added iodomethane. The mixture was refluxed for 1h and cooled to room temperature. Most of the solvent was removed in vacuo. The residue was added 100 mL water and stirred. The solid was filtered, washed with water, and dried to obtained the title compound (0.92g, 88.6%): ^{1}H NMR (300 MHz, $CDCl_3$) δ 7.95 (s, 1H), 7.50-7.30 (m, 10H), 6.57 (s, 1H), 5.12 (d, 4H), 3.88 (s, 3H); MS(ESI): 382.8$[M+H]^{+\cdot}$

3-(2,4-Bis(benzyloxy)-5-chlorophenyl)-2-(4-methoxyphenyl)-3-oxopropanenitrile (9). 4-Methoxybenzyl cyanide (0.2 g, 1.36 mmol) was added dropwise to LHMDS (3.4 mL, 3.4 mmol) in 20 mL dry tetrahydrofuran at -78 ^{o}C under N_2 protection. The mixture was stirred at -78 ^{o}C for 30 minutes and added compound **8** (0.5 g, 1.36 mmol) in 10 mL dry tetrahydrofuran dropwise. The mixture was kept stirring at -78 ^{o}C for 30 minutes and then 2 hours at room temperature. 10 mL 2M HCl was added to stop the reaction. Most of the solvent was removed in vacuo. The residue was extracted with dichloromethane. The organic layer was washed with brine, dried over Na_2SO_4 and evaporated in vacuo. The crude product was purified by flash chromatography on silica gel to afford the product as yellow oil (0.53g, 78.5%): ^{1}H NMR (300 MHz, $CDCl_3$) δ 7.74 (s, 1H), 7.63 (d, *J*=8.8Hz, 2H), 7.45-7.35 (m, 10H), 6.95 (d, *J*=8.8Hz, 2H), 6.65 (s, 1H) , 6.59 (s, 1H), 5.15 (s, 2H), 5.09 (s, 2H), 3.84 (s, 3H); MS (ESI): 496.1$[M-H]^-$.

3-(2,4-Bis(benzyloxy)-5-chlorophenyl)-4-(4-methoxyphenyl)isoxazol-5-amine (10). Compound **9** (0.15 g, 0.3 mmol) and hydroxylamine hydrochloride (0.042 g, 0.6 mmol) were dissolved in 5 mL dry pyridine and stirred at 100 ^{o}C overnight. The mixture was diluted with dichloromethane, washed with saturate citric acid/water (1:1, 30 mL×2), water (30mL×1), sat.$NaHCO_3$ (30mL×2), brine, dried over Na_2SO_4 and evaporated in vacuo. The crude product was purified by flash chromatography on silica gel to afford the product as white solid (0.1 g，68.6%): ^{1}H NMR (300

MHz, $CDCl_3$) δ 7.48 (s, 1H), 7.38-7.30 (m, 5H), 7.24-7.20 (m, 3H), 6.96 (d, *J*=8.6Hz, 2H), 6.89-6.84 (m, 2H), 6.78 (d, *J*=8.6Hz, 2H), 6.40 (s, 1H), 5.01 (s, 2H), 4.64 (s, 2H), 4.52 (s, 2H), 3.79 (s, 3H); MS (ESI): 513.1$[M+H]^+$.

General procedure for the synthesis of **23-35.** Compound **10** (0.2 g, 0.4 mmol) and triethylamine (1 mL) were dissolved in 20 mL dry dichloromethane. Catalytic amount of DMAP was added to the mixture followed by the addition of acyl chlorides (3 eq) dropwise. When stirred for 2 hours at room temperature, the mixture was diluted with dichloromethane. The organic layer was washed with saturate citric acid/water (1:1, 30 mL×2), water (30mL×1), sat.$NaHCO_3$ (30mL×2), brine, dried over Na_2SO_4 and evaporated in vacuo. The crude product was purified by flash chromatography on silica gel to afford the intermediates **11-22**. Compound **10-22** (1 eq) was dissolve in dry dichloromethane followed by addition of 1N BCl_3 in dichloromethane (3 eq) under nitrogen. The mixture was stirred for 2 hours at room temperature and then diluted with ethyl acetate. The organic layer was washed with sat.$NaHCO_3$ (30mL×2), brine, dried over Na_2SO_4 and evaporated in vacuo. The crude product was purified by flash chromatography on silica gel to afford the final product **23-35**.

4-(5-Amino-4-(4-methoxyphenyl)isoxazol-3-yl)-6-chlorobenzene-1,3-diol (23). White solid (70.9%): ^{1}H NMR (400MHz, CD_3OD) δ 7.13 (d, *J*=8.9Hz, 2H), 6.96 (s, 1H), 6.93 (d, *J*=8.9Hz, 2H), 6.44 (s, 1H), 3.79 (s, 3H); MS (ESI): 333.0$[M+H]^+$.

N-(3-(5-chloro-2,4-dihydroxyphenyl)-4-(4-methoxyphenyl)isoxazol-5-yl)acetamide (24). The intermediate **11** was obtained as white solid (88.6%): ^{1}H NMR (300 MHz, $CDCl_3$) δ 7.50 (s, 1H), 7.40-7.34 (m, 5H), 7.33 (s, 1H), 7.26-7.23 (m, 3H), 6.97 (d, *J*=8.6Hz, 2H), 6.85-6.90 (m, 2H), 6.78 (d, *J*=8.6Hz, 2H), 6.43 (s, 1H), 5.04 (s, 2H), 4.63 (s, 2H), 3.81 (s, 3H), 1.60 (s, 3H); MS(ESI): 555.1$[M+H]^+$. The title product was obtained as Amorphous white solid (56.4%): ^{1}H NMR (400MHz, CD_3OD) δ 7.13 (d, *J*=8.3Hz, 2H), 7.05 (s, 1H), 6.90 (d, *J*=8.3Hz, 2H), 6.45 (s, 1H), 3.77 (s, 3H) , 2.09 (s, 3H); MS (ESI): 375.0$[M+H]^+$.

N-(3-(5-chloro-2,4-dihydroxyphenyl)-4-(4-methoxyphenyl)isoxazol-5-yl)propionamide (25). Amorphous white solid (two steps totally 64.5%): ^{1}H NMR (400MHz, CD_3OD) δ 7.13 (d, *J*=8.4Hz, 2H), 7.04 (s, 1H), 6.89 (d, *J*=8.4Hz, 2H), 6.44 (s, 1H), 3.77 (s, 3H), 2.37 (t, *J*=7.4Hz, 2H), 1.13 (d, *J*=7.4Hz, 3H); MS (ESI): 389.0$[M+H]^+$.

N-(3-(5-chloro-2,4-dihydroxyphenyl)-4-(4-methoxyphenyl)isoxazol-5-yl)butyramide (26).

Amorphous white solid (two steps totally 58.8%): ^{1}H NMR (400MHz, CD_3OD) δ 7.13 (d, *J*=8.4Hz, 2H), 7.05 (s, 1H), 6.88 (d, *J*=8.4Hz, 2H), 6.45 (s, 1H), 3.77 (s, 3H), 2.32 (t, *J*=7.2Hz, 2H), 1.70-1.60 (m, 2H), 0.93 (t, *J*=7.2Hz, 3H); MS (ESI): 403.0$[M+H]^+$.

N-(3-(5-chloro-2,4-dihydroxyphenyl)-4-(4-methoxyphenyl)isoxazol-5-yl)isobutyramide (27). Amorphous white solid (two steps totally 57.7%): ^{1}H NMR (400MHz, CD_3OD) δ 7.12 (d, *J*=8.4Hz, 2H), 7.05 (s, 1H), 6.88 (d, *J*=8.4Hz, 2H), 6.45 (s, 1H), 3.77 (s, 3H), 2.66-2.58 (m, 1H), 1.14 (d, *J*=7.1Hz, 6H); MS (ESI): 403.0$[M+H]^+$.

N-(3-(5-chloro-2,4-dihydroxyphenyl)-4-(4-methoxyphenyl)isoxazol-5-yl)pivalamide (28). Amorphous white solid (two steps totally 58.4%): ^{1}H NMR (400MHz, CD_3OD) δ 7.12 (d, *J*=8.4Hz, 2H), 7.07 (s, 1H), 6.88 (d, *J*=8.4Hz, 2H), 6.45 (s, 1H), 3.77 (s, 3H), 1.23 (s, 9H); MS (ESI): 417.0$[M+H]^+$.

N-(3-(5-chloro-2,4-dihydroxyphenyl)-4-(4-methoxyphenyl)isoxazol-5-yl)-3-methylbutanamide (29). Amorphous white solid (two steps totally 61.5%): ^{1}H NMR (400MHz, CD_3OD) δ 7.14 (d, *J*=8.4Hz, 2H), 7.05 (s, 1H), 6.89 (d, *J*=8.4Hz, 2H), 6.45 (s, 1H), 3.77 (s, 3H), 2.22 (d, *J*=7.3Hz, 2H), 2.12-2.02 (m, 1H), 0.94 (d, *J*=6.7Hz, 6H); MS(ESI): 417.0$[M+H]^+$.

N-(3-(5-chloro-2,4-dihydroxyphenyl)-4-(4-methoxyphenyl)isoxazol-5-yl)cyclopropanecarboxamide (30). Amorphous white solid (two steps totally 49.1%): ^{1}H NMR (400MHz, CD_3OD) δ 7.13 (d, *J*=8.4Hz, 2H), 7.04 (s, 1H), 6.90 (d, *J*=8.4Hz, 2H), 6.44 (s, 1H), 3.78 (s, 3H), 1.76 (m, 1H), 0.94-0.85 (m, 4H); MS(ESI): 400.9$[M+H]^+$.

N-(3-(5-chloro-2,4-dihydroxyphenyl)-4-(4-methoxyphenyl)isoxazol-5-yl)cyclobutanecarboxamide (31). Amorphous white solid (two steps totally 34.8%): ^{1}H NMR (400MHz, CD_3OD) δ 7.12 (d, *J*=8.4Hz, 2H), 7.05 (s, 1H), 6.89 (d, *J*=8.4Hz, 2H), 6.45 (s, 1H), 3.78 (s, 3H), 2.32-2.14 (m, 5H), 2.06-1.96 (m, 1H), 1.92-1.82 (m, 1H); MS(ESI): 415.0$[M+H]^+$.

N-(3-(5-chloro-2,4-dihydroxyphenyl)-4-(4-methoxyphenyl)isoxazol-5-yl)cyclopentanecarboxamide (32). Amorphous white solid (two steps totally 62.6%): ^{1}H NMR (400MHz, CD_3OD) δ 7.13 (d, *J*=8.4Hz, 2H), 7.05 (s, 1H), 6.89 (d, *J*=8.4Hz, 2H), 6.45 (s, 1H), 3.77 (s, 3H), 2.86-2.77 (m, 1H), 1.94-1.83 (m, 2H), 1.80-1.67 (m, 4H), 1.63-1.55 (m, 2H); MS(ESI): 429.0$[M+H]^+$.

N-(3-(5-chloro-2,4-dihydroxyphenyl)-4-(4-methoxyphenyl)isoxazol-5-yl)cyclohexanecarboxamide (33). Amorphous white solid (two steps totally 70.2%): ^{1}H NMR (400MHz, CD_3OD) δ 7.12 (d, *J*=8.4Hz, 2H), 7.05 (s, 1H), 6.89 (d, *J*=8.4Hz, 2H), 6.45 (s, 1H), 3.78 (s, 3H), 2.41-2.32 (m,

1H), 1.87-1.75 (m, 4H), 1.50-1.38 (m, 2H), 1.37-1.20 (m, 4H); MS(ESI): 443.0$[M+H]^+$.

N-(3-(5-chloro-2,4-dihydroxyphenyl)-4-(4-methoxyphenyl)isoxazol-5-yl)octanamide (30). Amorphous white solid (two steps totally 70.0%): ^{1}H NMR (400MHz, CD_3OD) δ 7.13 (d, *J*=8.4Hz, 2H), 7.05 (s, 1H), 6.88 (d, *J*=8.4Hz, 2H), 6.45 (s, 1H), 3.77 (s, 3H), 2.34 (t, *J*=7.2Hz, 2H), 1.65-1.56 (m, 2H), 1.35-1.22 (m, 11H); MS(ESI): 459.0$[M+H]^+$.

1-(3-(5-Chloro-2,4-dihydroxyphenyl)-4-(4-methoxyphenyl)isoxazol-5-yl)-3-ethylurea (35). Amorphous white solid (two steps totally 26.2%): ^{1}H NMR (400MHz, CD_3OD) δ 7.16 (d, *J*=8.9Hz, 2H), 7.02 (s, 1H), 6.91 (d, *J*=8.9Hz, 2H), 6.45 (s, 1H), 3.78 (s, 3H), 3.16 (t, *J*=7.6Hz, 2H), 1.07 (d, *J*=7.6Hz, 3H); MS(ESI): 404.0$[M+H]^+$.

Compounds **41-45** were prepared according to the procedure of **9**.

3-(2,4-Bis(benzyloxy)-5-bromophenyl)-2-(4-methoxyphenyl)-3-oxopropanenitrile (41). Yellow oil (97.2%): MS (EI): 541,543$[M]^+$.

3-(2,4-Bis(benzyloxy)phenyl)-2-(4-methoxyphenyl)-3-oxopropanenitrile (42). Yellow oil (90.6%): ^{1}H NMR (300MHz, $CDCl_3$) δ 7.81 (d, *J*=8.8Hz, 1H), 7.47-7.33 (m, 10H), 7.05 (d, *J*=8.8Hz, 2H), 6.78 (d, *J*=8.8Hz, 2H), 6.64-6.57 (m, 2H), 5.80 (s, 1H), 5.19-5.05 (m, 4H), 3.76 (s, 3H); MS(EI): *m/z* 463$[M]^+$.

3-(2,4-Bis(benzyloxy)-5-ethylphenyl)-2-(4-methoxyphenyl)-3-oxopropanenitrile (43). Yellow oil (95.9%): ^{1}H NMR (400MHz, $CDCl_3$) δ 7.69 (s, 1H), 7.46-7.33 (m, 10H), 7.09 (d, *J*=8.7Hz, 2H), 6.79 (d, *J*=8.7Hz, 2H), 6.48 (s, 1H), 5.85 (s, 1H), 5.18-5.05 (m, 4H), 3.76 (s, 3H), 2.60 (q, *J* =7.8 Hz , 2H), 1.17 (t, *J* =7.8 Hz, 3H); MS(EI): 491$[M]^+$.

3-(2,4-Bis(benzyloxy)-5-isopropylphenyl)-2-(4-methoxyphenyl)-3-oxopropanenitrile (44). Yellow oil (90.4%): ^{1}H NMR (400MHz, $CDCl_3$) δ 7.76 (s, 1H), 7.46-7.33 (m, 10H), 7.10 (d, *J*=8.7Hz, 2H), 6.80 (d, *J*=8.7Hz, 2H), 6.48 (s, 1H), 5.84 (s, 1H), 5.20-5.04 (m, 4H), 3.76 (s, 3H), 3.24 (m, 1H), 1.20 (t, *J* = 6.5Hz, 6H); MS(EI): 505$[M]^+$.

3-(2,4-Bis(benzyloxy)-5-(tert-butyl)phenyl)-2-(4-methoxyphenyl)-3-oxopropanenitrile (45). Yellow oil (88%): ^{1}H NMR (400MHz, $CDCl_3$) δ 7.85 (s, 1H), 7.45-7.34 (m, 10H), 7.11 (d, *J*=8.7Hz, 2H), 6.80 (d, *J*=8.7Hz, 2H), 6.49 (s, 1H), 5.83 (s, 1H), 5.20-5.07 (m, 4H), 3.77 (s, 3H), 1.34 (s, 9H); MS(EI): 519$[M]^+$.

Compounds **46-50** were prepared according to the procedure of **10**.

3-(2,4-Bis(benzyloxy)-5-bromophenyl)-4-(4-methoxyphenyl)isoxazol-5-amine (46). Yellow

solid (54.7%): ^{1}H NMR (300 MHz, $CDCl_3$) δ 7.67 (s, 1H), 7.40-7.35 (m, 5H), 7.26-7.21 (m, 3H), 6.98 (d, *J*=8.6Hz, 2H), 6.90-6.86 (m, 2H), 6.79 (d, *J*=8.6Hz, 2H), 6.40 (s, 1H), 5.02 (s, 2H), 4.66 (s, 2H), 4.54 (s, 2H), 3.80 (s, 3H); MS(ESI): 557.0$[M+H]^+$.

3-(2,4-Bis(benzyloxy)phenyl)-4-(4-methoxyphenyl)isoxazol-5-amine (47). Yellow oil (17.8%): ^{1}H NMR (300MHz, $CDCl_3$) δ 7.45-7.32 (m, 6H), 7.25-7.19 (m, 3H), 7.00-6.92 (m, 4H), 6.77 (d, *J*=8.8Hz, 2H), 6.62 (dd, *J*=1.3, 8.8Hz, 1H), 6.48 (d, *J*=2.0Hz, 1H), 5.01 (s, 2H), 4.72 (s, 2H), 4.52 (s, 2H), 3.78 (s, 3H); MS(ESI): 479.0$[M+H]^+$.

3-(2,4-Bis(benzyloxy)-5-ethylphenyl)-4-(4-methoxyphenyl)isoxazol-5-amine (48). Yellow oil (36.9%): ^{1}H NMR (300MHz, $CDCl_3$) δ 7.41-7.30 (m, 6H), 7.24-7.20 (m, 3H), 6.99 (d, *J*=8.9Hz, 2H), 6.96-6.91 (m, 2H), 6.78 (d, *J*=8.9Hz, 2H), 6.39 (s, 1H), 4.95 (s, 2H), 4.67 (s, 2H), 4.50 (s, 2H), 3.78 (s, 3H), 2.63 (q, *J* =7.8 Hz , 2H), 1.18 (t, *J* =7.8 Hz, 3H); MS(ESI): 507.0$[M+H]^+$.

3-(2,4-Bis(benzyloxy)-5-isopropylphenyl)-4-(4-methoxyphenyl)isoxazol-5-amine (49). ellow oil (37.1%): ^{1}H NMR (300MHz, $CDCl_3$) δ 7.40-7.30 (m, 5H), 7.27 (s, 1H), 7.23-7.21 (m, 3H), 6.97 (d, *J*=8.1Hz, 2H), 6.96-6.92 (m, 2H), 6.78 (d, *J*=8.1Hz, 2H), 6.38 (s, 1H), 4.94 (s, 2H), 4.68 (s, 2H), 4.49 (s, 2H), 3.78 (s, 3H), 3.29 (m, 1H), 1.18 (d, 6H); MS(ESI): 521.0$[M+H]^+$.

3-(2,4-Bis(benzyloxy)-5-(tert-butyl)phenyl)-4-(4-methoxyphenyl)isoxazol-5-amine (50). Yellow solid (21.3%): ^{1}H NMR (300MHz, $CDCl_3$) δ 7.39-7.36 (m, 5H), 7.32 (s, 1H), 7.24-7.21 (m, 3H), 6.99 (d, *J*=8.6Hz, 2H), 6.96-6.92 (m, 2H), 6.79 (d, *J*=8.6Hz, 2H), 6.40 (s, 1H), 4.96 (s, 2H), 4.68 (s, 2H), 4.49 (s, 2H), 3.79 (s, 3H), 1.33 (d, 9H); MS(ESI): 535.0$[M+H]^+$.

Compounds **51-55** were prepared according to the procedure of **11-22**.

N-acetyl-N-(3-(2,4-bis(benzyloxy)-5-bromophenyl)-4-(4-methoxyphenyl)isoxazol-5-yl)acetamide (51). Yellow solid (90%): 1H NMR (400 MHz, CDCl3) δ 7.71 (s, 1H), 7.41-7.33 (m, 5H), 7.27-7.19 (m, 3H), 7.00-6.86 (m, 4H), 6.76-6.70 (m, 2H), 6.44 (s, 1H), 5.07 (s, 2H), 4.62 (s, 2H), 3.77 (s, 3H), 2.15-1.93 (m, 2H), 1.07-0.98 (m, 4H) , 0.87-0.77 (m, 4H); MS(EI): 692,694[M]+.

N-acetyl-N-(3-(2,4-bis(benzyloxy)phenyl)-4-(4-methoxyphenyl)isoxazol-5-yl)acetamide (52). Yellow solid (74%): ^{1}H NMR (300MHz, $CDCl_3$) δ 7.45-7.32 (m, 6H), 7.25-7.19 (m, 3H), 7.00-6.92 (m, 4H), 6.77 (d, *J*=8.8Hz, 2H), 6.62 (dd, *J*=1.3, 8.8Hz, 1H), 6.48 (d, *J*=2.0Hz, 1H), 5.01 (s, 2H), 4.72 (s, 2H), 3.78 (s, 3H) , 2.25 (s, 6H); MS(EI): 562$[M]^+$.

N-acetyl-N-(3-(2,4-bis(benzyloxy)-5-ethylphenyl)-4-(4-methoxyphenyl)isoxazol-5-yl)acetamide (53). Yellow solid (76.3%): ^{1}H NMR (300MHz, $CDCl_3$) δ 7.41-7.36 (m, 5H), 7.30 (s, 1H),

7.25-7.22 (m, 3H), 7.00-6.96 (m, 2H), 6.87 (d, *J*=8.7Hz, 2H), 6.72 (d, *J*=8.7Hz, 2H), 6.45 (s, 1H), 5.01 (s, 2H), 4.66 (s, 2H), 3.76 (s, 3H), 2.66 (q, *J* =7.8 Hz , 2H), 2.26 (s, 6H), 1.21 (d, *J*=7.8Hz, 3H); MS(EI): 590$[M]^+$.

N-acetyl-N-(3-(2,4-bis(benzyloxy)-5-(tert-butyl)phenyl)-4-(4-methoxyphenyl)isoxazol-5-yl)acetamide (54). Yellow solid (80.4%): MS(EI): 618$[M]^+$.

Compounds **56-59** were prepared according to the procedure of **23-35**.

N-(3-(5-bromo-2,4-dihydroxyphenyl)-4-(4-methoxyphenyl)isoxazol-5-yl)acetamide (56). Amorphous white solid (36.7%): ^{1}H NMR (400MHz, CD_3OD) δ 7.20 (s, 1H), 7.13 (d, *J*=8.4Hz, 2H), 6.90 (d, *J*=8.4Hz, 2H), 6.44 (s, 1H), 3.78 (s, 3H), 2.08 (s, 3H); MS(ESI): 420.9$[M+H]^+$.

N-(3-(2,4-dihydroxyphenyl)-4-(4-methoxyphenyl)isoxazol-5-yl)acetamide (57). White solid (77.7%): ^{1}H NMR (400MHz, CD_3OD) δ 7.13 (d, *J*=8.7Hz, 2H), 6.93 (d, *J*=8.9Hz, 1H), 6.87 (d, *J*=8.7Hz, 2H), 6.32 (d, *J*=2.5Hz, 1H), 6.23 (dd, *J*=2.5, 8.9Hz, 1H), 3.76(s, 3H), 2.08 (s, 3H); MS(ESI): 341.0$[M+H]^+$.

N-(3-(5-ethyl-2,4-dihydroxyphenyl)-4-(4-methoxyphenyl)isoxazol-5-yl)acetamide (58). Amorphous white solid (59.5%): ^{1}H NMR (400MHz, CD_3OD) δ 7.16 (d, *J*=8.4Hz, 2H), 6.91 (d, *J*=8.4Hz, 2H), 6.78 (s, 1H), 6.33 (s, 1H), 3.79 (s, 3H), 2.36 (q, *J*=7.3Hz, 2H), 2.08 (s, 3H), 0.94 (t, *J*=7.3Hz, 3H); MS(ESI): 369.0$[M+H]^+$.

N-(3-(5-(tert-butyl)-2,4-dihydroxyphenyl)-4-(4-methoxyphenyl)isoxazol-5-yl)acetamide (59). Amorphous white solid (87.4%): ^{1}H NMR (400MHz, CD_3OD) δ 7.17 (d, *J*=8.4Hz, 2H), 6.95 (d, *J*=8.4Hz, 2H), 6.90 (s, 1H), 6.33 (s, 1H), 3.80 (s, 3H), 2.07 (s, 3H), 1.09 (s, 9H); MS(ESI): 397.0$[M+H]^+$.

N-(3-(2,4-dihydroxy-5-isopropylphenyl)-4-(4-methoxyphenyl)isoxazol-5-yl)cyclopropanecarboxamide (60). Compound **49** (0.2 g, 0.4 mmol) and triethylamine (1.13 mL, 8 mmol) were dissolved in 20 mL dry dichloromethane. Catalytic amount of DMAP was added to the mixture followed by the addition of cyclopropylcarboxyl chloride (0.21 mg, 2 mmol) dropwise. When stirred for 2 hours at room temperature, the mixture was diluted with dichloromethane. The organic layer was washed with saturate citric acid/water (1:1, 30 mL×2), water (30mL×1), sat.$NaHCO_3$ (30mL×2), brine, dried over Na_2SO_4 and evaporated in vacuo. The crude product was purified by flash chromatography on silica gel to afford the intermediates **55**. Compound **55** (0.1 g, 0.16 mmol) was dissolve in dry dichloromethane (20 mL) followed by addition of 1N BCl_3 in

dichloromethane (0.5 mL) under nitrogen. The mixture was stirred for 2 hours at room temperature and then diluted with ethyl acetate. The organic layer was washed with sat.$NaHCO_3$ (30mL×2), brine, dried over Na_2SO_4 and evaporated in vacuo. The crude product was purified by flash chromatography on silica gel to afford the final product **60** (two steps totally 47.6%): ^{1}H NMR (400MHz, CD_3OD) δ 7.16 (d, *J*=8.2Hz, 2H), 6.94 (d, *J*=7.8Hz, 2H), 6.81 (s, 1H), 6.33 (s, 1H), 3.79 (s, 3H), 3.03 (m, 1H), 1.75 (m, 1H), 0.90 (d, 10H); MS(ESI): 409.1$[M+H]^+$.

1-(2,4-Bis(benzyloxy)phenyl)ethanone (62). Benzyl bromide (483 mL, 4 mol) was added to the suspension of 2,4-dihydroxyacetophenone (280 g, 1.84 mol) and potassium carbonate anhydrous (560 g, 4 mol) in acetonitrile (1.4 L) dropwise. The mixture was refluxed overnight and cooled to ambient temperature. Most of the solvent was removed in vacuo. The residue was added water (2 L) and stirred at room temperature. White solid was formed. The solid was filtered, washed with water followed by petroleum and dried to yield title compound as white solid (590 g, 96.5%): ^{1}H NMR (300 MHz, $CDCl_3$) δ 7.85 (d, *J*=9.3Hz, 1H), 7.44-7.35 (m, 10H), 6.63-6.60 (m, 2H), 5.11 (s, 2H), 5.08 (s, 2H), 2.55 (s, 3H); MS(EI): 332$[M]^+$.

(((4-(Prop-1-en-2-yl)-1,3-phenylene)bis(oxy))bis(methylene))dibenzene (63). Methyltriphenylphosphonium bromide (826 g, 2.31 mol) was suspended in dry tetrahydrofuran under nitrogen. The suspension was cooled to -5 ^{o}C and added 2.5 M n-Butyllithium in hexanes (924 mL, 2.31 mol). After stirred for 0.5 hour the mixture was added compound **62** (590 g, 1.78 mol) in dry tetrahydrofuran and stirred for another 0.5 hour at -5 ^{o}C. The mixture was warmed to ambient temperature and stirred overnight. Methanol was added to stop the reaction. The solvent was removed in vacuo. The residue was separated in hexane and water. The organic layer was concentrated. The crude product was purified by flash chromatography on silica gel to afford the final product as white wax (466g, 79.5%): ^{1}H NMR (300MHz, $CDCl_3$) δ 7.44-7.29 (m, 10H), 7.14 (d, *J*=8.3Hz, 1H), 6.59 (d, *J*=2.5Hz, 1H), 6.54 (m, 1H), 5.07 (s, 2H), 5.05 (s,2H), 5.03 (s, 2H), 2.12 (s, 3H); MS(EI): 330$[M]^+$.

4-Isopropylbenzene-1,3-diol (64). Compound **63** (466 g, 1.4 mol) was dissolved in mixed solvent of dichloromethane/ethanol (1:50, v/v), followed the addition of 10% palladium on carbon (100 g). The mixture was stirred at 60 ^{o}C under 20 atm. hydrogen pressures for 8 hours. The mixture was filtered, concentrated and purified by flash chromatography on silica gel to afford the final product as white solid (178 g, 82.9%): ^{1}H NMR (300 MHz,$CDCl_3$) δ 7.03 (d, *J*=8.3Hz, 1H), 6.38 (d,

J=8.3Hz 1H), 6.29 (d, *J*=2.5Hz, 1H), 4.74 (brs, 1H), 4.63 (brs, 1H), 3.09 (m,1H), 1.22 (d, 6H); MS(EI): 152$[M]^+$.

2,4-Dihydroxy-5-isopropylbenzaldehyde (65). Phosphorus oxychloride (155 mL, 1.64 mol) was added to 350 mL dry dimethylformamide at -5 ^oC and stirred for 0.5 hour. The mixture was added compound **64** (100g, 0.65mol) in 200 mL dry dimethylformamide and stirred at room temperature for 1 hour and at 50 ^oC for another 1 hour. After cooled down the mixture was poured into sodium hydroxide (315 g) in 2 L water slowly and stirred at 70 ^oC for 15 minutes. The mixture was cooled to room temperature and acidified to pH 2-3 by concentrated HCl. The aqueous layer was extracted with ethyl acetate. The organic layer was washed with brine, dried over Na_2SO_4, concentrated and purified by flash chromatography on silica gel to afford the final product as white solid (86.65 g, 73.2%): ^{1}H NMR(300MHz, $CDCl_3$) δ 11.29 (s, 1H), 9.70 (s, 1H), 7.34 (s, 1H), 6.60 (s, 1H), 6.36 (s, 1H), 3.18 (m, 1H), 1.26 (d, 6H); MS(EI): 180$[M]^+$.

2,4-Bis(benzyloxy)-5-isopropylbenzaldehyde (66). Compound **66** was prepared according to the procedure of **62** (82.7%): ^{1}H NMR(300MHz, $CDCl_3$) δ 10.40 (s, 1H), 7.76 (s, 1H), 7.43-7.33 (s, 10H), 6.52 (s, 1H), 6.36 (s, 1H), 5.13 (s, 2H), 5.11 (s, 2H), 3.29 (m, 1H), 1.23 (d, 6H); MS(EI): 360$[M]^+$.

(2,4-Bis(benzyloxy)-5-isopropylbenzaldehyde oxime (67). Compound **66** (143.2 g, 0.4 mol), hydroxylamine hydrochloride (55.5 g, 0.8 mol) and sodium hydroxide (32 g, 0.8 mol) were suspended in the mixture of ethanol 600 mL and water 300 mL. The mixture was stirred at 100 ^oC for 5 hours and cooled to room temperature. Most of the solvent was removed in vacuo. The residue was added 2 L water and stirred for 0.5 hour. The precipitant was filtered, washed with water and petroleum and dried to yield the title compound as white solid (140.1 g, 93.9%): ^{1}H NMR(300MHz, $CDCl_3$) δ 8.51 (s, 1H), 7.62 (s, 1H), 7.41-7.31 (s, 10H), 6.51 (s, 1H), 5.05 (d, 4H) , 3.30 (m, 1H), 1.22 (d, 6H); MS(EI): 375$[M]^+$.

4-(Cyanomethyl)benzoic acid (70). Methyl 4-(cyanomethyl)benzoate (25 g, 0.14 mol) dissolved in 300 mL methanol was add 160 mL 1 N NaOH and refluxed for3 hours. Most of the solvent was removed in vacuo. The residue was added 500 mL water and acidified to pH 2-3 with concentrated HCl. The generated solid was filtered, washed with water and dried to give the title compound as white solid (21.2 g, 92.2%): ^{1}H NMR (400 MHz, DMSO-d_6) δ 12.89 (brs, 1H), 7.87 (d, *J*=8.2Hz, 2H), 7.37 (d, *J*=8.2Hz, 2H), 3.45 (s, 2H); MS(EI): 161$[M]^+$.

2-(4-(Hydroxymethyl)phenyl)acetonitrile (71). 1,1'-Carbonyldiimidazole (23.3 g, 0.14 mol) was added to compound **70** (21.2 g, 0.13 mol) in 600 mL dry tetrahydrofuran portion-wise. The mixture was stirred at room temperature till no bubble was observed. The mixture was added sodium borohydride (15 g, 0.39 mol) in 800 mL water dropwise and stirred at room temperature for 4 hours. The mixture was extracted with ethyl acetate. The organic layer was washed with brine, dried over Na_2SO_4, concentrated and purified by flash chromatography on silica gel to afford the final product as colorless oil (14.36 g, 74.2%): ^{1}H NMR(300MHz, $CDCl_3$) δ 7.37 (d, *J*=8.5Hz, 2H), 7.30 (d, *J*=8.5Hz, 2H), 4.68 (s, 2H), 3.74 (s, 2H); MS(EI): 147$[M]^+$.

2-(4-(((Tetrahydro-2H-pyran-2-yl)oxy)methyl)phenyl)acetonitrile (72). Compound **71** (14.36 g, 98 mmol), 3,4-Dihydro-2H-pyran (10.05 mL, 110 mmol) and p-toluenesulfonic acid monohydrate (0.345 g, 1.8 mmol) were dissolved in 400 mL dichloromethane and stirred at room temperature for 1 hour. The mixture was diluted with dichloromethane, washed with saturated sodium bicarbonate (300 mL×2), brine (300 mL), dried over Na_2SO_4, concentrated and purified by flash chromatography on silica gel to afford the final product as colorless oil (20.11 g, 89.1%): ^{1}H NMR(300MHz, $CDCl_3$) δ 7.38 (d, *J*=8.3Hz, 2H), 7.30 (d, *J*=8.3Hz, 2H), 4.78 (d, *J*=11.2Hz, 1H), 4.69 (t, *J*=3.4Hz, 1H), 4.49 (d, *J*=11.2Hz, 1H), 3.93-3.87 (m, 1H), 3.74 (s, 2H), 3.58-3.51 (m, 1H), 1.90-1.80 (m, 1H), 1.78-1.70 (m, 1H), 1.68-1.51 (m, 4H); MS(EI): 231$[M]^+$.

3-(2,4-Bis(benzyloxy)-5-isopropylphenyl)-4-(4-(((tetrahydro-2H-pyran-2-yl)oxy)methyl)phenyl)isoxazol-5-amine (73). Compound **67** (140 g, 0.37 mol) dissolved in 500 mL dry dimethylformamide was added N- chlorosuccinimide (60 g, 0.45 mol). After stirred at room temperature for 5 hours, the mixture was diluted with dichloromethane, washed with brine, dried over Na_2SO_4 and concentrated. The crude product of compound **68** was unstable and used immediately in the next step without further purification. Compound **72** (180 mg, 0.78 mmol) dissolved in 300 mL dry tetrahydrofuran was added tert-butyllithium (1.6 M in pentane, 1 mL, 1.6 mmmol) at -78 ^{o}C under nitrogen and stirred for 20 minutes followed by the addition of compound **68** (320 mg, 0.78 mmol) in 100 mL dry tetrahydrofuran. The mixture was kept stirring at -78 ^{o}C for 30 minutes and added 50 mL water to stop the reaction. Most of the tetrahydrofuran was removed and the residue was extracted with dichloromethane. The organic layer was washed with brine, dried over Na_2SO_4, concentrated and purified by flash chromatography on silica gel to afford the final product as yellow solid (286 mg, 60.7%). ^{1}H NMR(300MHz, $CDCl_3$) δ 7.40-7.19

(m, 11H), 7.03 (d, *J*=8.1Hz, 2H), 6.92-6.88 (m, 2H), 6.39 (s, 1H), 4.94 (s, 2H), 4.77 (d, *J*=11.9Hz, 1H), 4.72 (t, *J*=3.4Hz, 1H), 4.65 (s, 2H), 4.58 (s, 2H), 4.46 (d, *J*=11.9Hz, 1H), 3.97-3.89 (m, 1H), 3.60-3.53 (m, 1H), 3.30 (m, 1H), 1.92-1.81 (m, 1H), 1.79-1.71 (m, 1H), 1.69-1.51 (m, 4H), 1.18 (d, 6H).

N-(3-(2,4-bis(benzyloxy)-5-isopropylphenyl)-4-(4-(((tetrahydro-2H-pyran-2-yl)oxy)methyl)phenyl)isoxazol-5-yl)-N-(cyclopropanecarbonyl)cyclopropanecarboxamide (74). Compound **73** (0.2 g, 0.33 mmol) and triethylamine (1.13 mL, 8 mmol) were dissolved in 100 mL dry dichloromethane. Catalytic amount of DMAP was added to the mixture followed by the addition of cyclopropylcarboxyl chloride (0.21 mg, 2 mmol) dropwise. When stirred for 2 hours at room temperature, the mixture was diluted with dichloromethane. The organic layer was washed with saturate citric acid/water (1:1, 30 mL×2), water (30mL×1), sat.$NaHCO_3$ (30mL×2), brine, dried over Na_2SO_4 and evaporated in vacuo. The crude product was purified by flash chromatography on silica gel to afford title compound as yellow solid (204 mg, 83.3%): ^{1}H NMR(300MHz, $CDCl_3$) δ 7.42-7.32 (m, 6H), 7.25-7.19 (m, 5H), 7.03 (d, *J*=7.8Hz, 2H), 6.98-6.93 (m, 2H), 6.46 (s, 1H), 5.01 (s, 2H), 4.77 (d, *J*=12.5Hz, 1H), 4.71 (t, *J*=3.6Hz, 1H), 4.65 (s, 2H), 4.47 (d, *J*=12.1Hz, 1H), 3.96-3.88 (m, 1H), 3.60-3.51 (m, 1H), 3.30 (m, 1H), 1.91-1.52 (m, 8H), 1.21 (d, 6H), 0.98-0.92 (m, 4H), 0.87-0.82 (m, 4H); MS(ESI): 741.3$[M+H]^+$.

N-(3-(2,4-bis(benzyloxy)-5-isopropylphenyl)-4-(4-(hydroxymethyl)phenyl)isoxazol-5-yl)-N-(cyclopropanecarbonyl)cyclopropanecarboxamide (75). Compound **74** (2g, 2.7mmol) and p-toluenesulfonic acid monohydrate (0.05 g, 0.27 mmol) was dissolved in methanol 100 mL and tetrahydrofuran 100 mL and stirred at room temperature for 1 hour. The mixture was diluted with dichloromethane, washed with saturated sodium bicarbonate (100 mL×2), brine (100 mL), dried over Na_2SO_4, concentrated and purified by flash chromatography on silica gel to afford the final product as yellow solid (1.325 g, 74.7%). ^{1}H NMR(300MHz, $CDCl_3$) δ 7.42-7.33 (m, 6H), 7.26-7.18 (m, 5H), 7.03 (d, *J*=8.1Hz, 2H), 6.99-6.95 (m, 2H), 6.46 (s, 1H), 5.02 (s, 2H), 4.66 (s, 4H), 3.30 (m, 1H), 2.10-2.00 (m, 2H), 1.22 (d, 6H), 1.08-1.02 (m, 4H), 0.88-0.81 (m, 4H); MS(EI): 656$[M]^+$.

4-(3-(2,4-Bis(benzyloxy)-5-isopropylphenyl)-5-(cyclopropanecarboxamido)isoxazol-4-yl)benzyl methanesulfonate (76). Compound **75** (200mg, 0.3mmol) and triethylamine (1.13 mL, 8 mmol) dissolved in dry dichloromethane was added methanesulfonyl chloride (0.116 mL, 1.5 mmol) and

stirred at room temperature for 2 hours. The mixture was diluted with dichloromethane, washed with saturate citric acid/water (1:1, 100 mL×2), water (100mL×1), sat.$NaHCO_3$ (100mL×2), brine, dried over Na_2SO_4 and concentrated to give the title compound as pale-yellow solid (134mg, 67.7%). The compound was used without purification.

General procedure for the synthesis of **93-108**. Compound **76** (1 mmol) and amines (2.5 eq) were dissolved in 20 mL acetonitrile and stirred overnight at room temperature. The mixture was concentrated and added 50 mL water. The aqueous layer was extracted with dichloromethane. The organic layer was washed with brine, dried over Na_2SO_4 and concentrated to give **77-92** without purification. Compound **77-92** (1 eq) was dissolve in dry dichloromethane followed by addition of 1N BCl_3 in dichloromethane (3 eq) under nitrogen. The mixture was stirred for 2 hours at room temperature and then diluted with ethyl acetate. The organic layer was washed with sat.$NaHCO_3$, brine, dried over Na_2SO_4 and evaporated in vacuo. The crude product was purified by flash chromatography on silica gel to afford the final product **93-108**.

N-(3-(2,4-dihydroxy-5-isopropylphenyl)-4-(4-(morpholinomethyl)phenyl)isoxazol-5-yl)cyclopropanecarboxamide (93). White solid (44.1%): ^{1}H NMR (400MHz, CD_3OD) δ 7.39 (d, *J*=7.8Hz, 2H), 7.25 (d, *J*=7.8Hz, 2H), 6.80 (s, 1H), 6.33 (s, 1H), 3.71 (t, *J*=4.5Hz, 4H), 3.67 (s, 2H), 3.03 (m, 1H), 2.60 (brs, 4H), 1.74 (m, 1H), 0.89 (m, 10H); ^{13}C NMR (100MHz, d^6-DMSO) δ 173.0, 161.5, 157.3, 156.7, 154.0, 131.3, 131.2, 128.1, 127.8, 127.6, 125.4, 110.0, 106.3, 102.6, 66.4, 63.0, 58.6, 50.6, 25.6, 22.6, 7.9; MS(ESI): 478.2$[M+H]^+$; HRMS calcd for $C_{27}H_{32}N_3O_5$: 478.2342 $(M+H)^+$ Found: 478.2338.

N-(3-(2,4-dihydroxy-5-isopropylphenyl)-4-(4-(piperidin-1-ylmethyl)phenyl)isoxazol-5-yl)cyclopropanecarboxamide (94). White solid (29.4%): ^{1}H NMR (400MHz, CD_3OD) δ 7.47 (d, *J*=8.2Hz, 2H), 7.32 (d, *J*=8.2Hz, 2H), 6.82 (s, 1H), 6.32 (s, 1H), 4.13 (s, 2H), 3.10-3.01 (m, 5H), 1.83-1.73 (m, 5H), 1.63 (brs, 2H), 0.95 (m, 6H), 0.87 (m, 4H); MS(ESI): 476.2$[M+H]^+$.

N-(4-(4-((diethylamino)methyl)phenyl)-3-(2,4-dihydroxy-5-isopropylphenyl)isoxazol-5-yl)cyclopropanecarboxamide (95). White solid (38.8%): ^{1}H NMR (400MHz, CD_3OD) δ 7.49 (d, *J*=7.9Hz, 2H), 7.34 (d, *J*=7.9Hz, 2H), 6.84 (s, 1H), 6.33 (s, 1H), 4.24 (s, 2H), 3.15-3.03 (m, 5H), 1.76 (m, 1H), 1.30 (t, *J*=7.3Hz, 6H), 0.97 (d, *J*=6.7Hz, 6H), 0.88 (d, *J*=6.0Hz, 4H); MS(ESI): 464.1$[M+H]^+$.

N-(3-(2,4-dihydroxy-5-isopropylphenyl)-4-(4-((4-methylpiperazin-1-yl)methyl)phenyl)isoxaz

ol-5-yl)cyclopropanecarboxamide (96). White solid (28.5%): ^{1}H NMR (400MHz, CD_3OD) δ 7.37 (d, *J*=8.2Hz, 2H), 7.24 (d, *J*=8.2Hz, 2H), 6.80 (s, 1H), 6.34 (s, 1H), 3.60 (s, 2H), 3.04 (m, 1H), 2.92 (brs, 4H), 2.64 (brs, 4H), 2.60 (s, 3H), 1.75 (m, 1H), 0.92-0.85 (m, 10H); MS(ESI): 491.3$[M+H]^+$.

N-(3-(2,4-dihydroxy-5-isopropylphenyl)-4-(4-(thiomorpholinomethyl)phenyl)isoxazol-5-yl)cyclopropanecarboxamide (97). White solid (36.4%): ^{1}H NMR (400MHz, CD_3OD) δ 7.35 (d, *J*=8.3Hz, 2H), 7.22 (d, *J*=8.3Hz, 2H), 6.80 (s, 1H), 6.34 (s, 1H), 3.56 (s, 2H), 3.03 (m, 1H), 2.75-2.71 (m, 4H), 2.67-2.63 (m, 4H), 1.74 (m, 1H), 0.91-0.85 (m, 10H); MS(ESI): 494.2$[M+H]^+$.

N-(3-(2,4-dihydroxy-5-isopropylphenyl)-4-(4-((diisopropylamino)methyl)phenyl)isoxazol-5-yl)cyclopropanecarboxamide (98). White solid (36.6%): ^{1}H NMR (400MHz, CD_3OD) δ 7.47 (d, *J*=8.1Hz, 2H), 7.30 (d, *J*=8.1Hz, 2H), 6.84 (s, 1H), 6.32 (s, 1H), 4.20 (brs, 2H), 3.58 (brs, 2H), 3.06 (m, 1H), 1.75 (m, 1H), 1.36-1.26 (m, 12H), 0.96 (d, 6H), 0.87 (d, 4H); MS(ESI): 492.2$[M+H]^+$.

N-(3-(2,4-dihydroxy-5-isopropylphenyl)-4-(4-((methyl(phenethyl)amino)methyl)phenyl)isoxazol-5-yl)cyclopropanecarboxamide (99). White solid (24.7%): ^{1}H NMR (400MHz, CD_3OD) δ 7.37 (d, *J*=8.2Hz, 2H), 7.29-7.24 (m, 4H), 7.21-7.16 (m, 3H), 6.82 (s, 1H), 6.33 (s, 1H), 3.81 (s, 2H), 3.02 (m, 1H), 2.93-2.80 (m, 4H), 2.45 (s, 3H), 1.74 (m, 1H), 0.92-0.86 (m, 10H); MS(ESI): 526.3$[M+H]^+$.

N-(4-(4-((3,4-dihydroisoquinolin-2(1H)-yl)methyl)phenyl)-3-(2,4-dihydroxy-5-isopropylphenyl)isoxazol-5-yl)cyclopropanecarboxamide (100). White solid (28.6%): ^{1}H NMR (400MHz, CD_3OD) δ 7.44 (d, *J*=7.7Hz, 2H), 7.26 (d, *J*=7.7Hz, 2H), 7.12-7.09 (s, 3H), 7.01-6.97 (s, 1H), 6.82 (s, 1H), 6.34 (s, 1H), 3.76 (s, 2H), 3.68 (s, 2H), 3.02 (m, 1H), 2.91 (t, *J*=5.8Hz, 2H), 2.81 (t, *J*=5.4Hz, 2H), 1.75 (m, 1H), 0.92-0.84 (m, 10H); MS(ESI): 524.3$[M+H]^+$.

N-(3-(2,4-dihydroxy-5-isopropylphenyl)-4-(4-((2,6-dimethylmorpholino)methyl)phenyl)isoxazol-5-yl)cyclopropanecarboxamide (101). White solid (25.7%): ^{1}H NMR (400MHz, CD_3OD) δ 7.36 (d, *J*=8.3Hz, 2H), 7.23 (d, *J*=8.3Hz, 2H), 6.81 (s, 1H), 6.34 (s, 1H), 3.72-3.64 (m, 2H), 3.54 (s, 2H), 3.03 (m, 1H), 2.77 (d, *J*=10.7Hz, 2H), 1.82-1.71 (m, 3H), 1.11 (d, 6H), 0.91-0.85 (m, 10H); MS(ESI): 506.3$[M+H]^+$.

N-(3-(2,4-dihydroxy-5-isopropylphenyl)-4-(4-((3,5-dimethylpiperidin-1-yl)methyl)phenyl)isoxazol-5-yl)cyclopropanecarboxamide (102). White solid (33.7%): ^{1}H NMR (400MHz, CD_3OD)

δ 7.43 (d, *J*=8.4Hz, 2H), 7.29 (d, *J*=8.4Hz, 2H), 6.83 (s, 1H), 6.34 (s, 1H), 3.93 (s, 2H), 3.12-3.03 (m, 3H), 2.08-2.01 (m, 2H), 1.86-1.74 (m, 5H), 0.95-0.86 (m, 16H); MS(ESI): 502.3$[M+H]^+$.

N-(3-(2,4-dihydroxy-5-isopropylphenyl)-4-(4-((2-methylpiperidin-1-yl)methyl)phenyl)isoxazol-5-yl)cyclopropanecarboxamide (103). White solid (42.9%): ^{1}H NMR (400MHz, CD_3OD) δ 7.46 (d, *J*=8.1Hz, 2H), 7.32 (d, *J*=8.1Hz, 2H), 6.83 (s, 1H), 6.33 (s, 1H), 4.44 (d, *J*=12.9Hz, 1H), 3.87 (d, *J*=12.9Hz, 1H), 3.13-3.02 (m, 3H), 2.69-2.61 (m, 1H), 1.93-1.86 (m, 1H), 1.82-1.72 (m, 3H), 1.69-1.57 (m, 2H), 1.54-1.42 (m, 4H), 0.95 (d, 6H), 0.88 (d, 4H); MS(ESI): 490.3$[M+H]^+$.

N-(3-(2,4-dihydroxy-5-isopropylphenyl)-4-(4-((4-(dimethylamino)piperidin-1-yl)methyl)phenyl)isoxazol-5-yl)cyclopropanecarboxamide (104). White solid (34.7%): ^{1}H NMR (400MHz, CD_3OD) δ 7.36 (d, *J*=8.2Hz, 2H), 7.24 (d, *J*=8.2Hz, 2H), 6.79 (s, 1H), 6.34 (s, 1H), 3.61 (s, 2H), 3.20-2.99 (m, 4H), 2.82 (s, 6H), 2.18 (t, *J*=12.4Hz, 2H), 2.06 (d, *J*=10Hz, 2H), 1.80-1.68 (m, 3H), 0.95-0.83 (m, 10H); MS(ESI): *m/z* 519.3$[M+H]^+$.

N-(3-(2,4-dihydroxy-5-isopropylphenyl)-4-(4-(((2-(dimethylamino)ethyl)(methyl)amino)methyl)phenyl)isoxazol-5-yl)cyclopropanecarboxamide (105). White solid (34.5%): ^{1}H NMR (400MHz, CD_3OD) δ 7.43 (d, *J*=7.6Hz, 2H), 7.26 (d, *J*=7.6Hz, 2H), 6.84 (s, 1H), 6.33 (s, 1H), 3.74 (brs, 2H), 3.13-3.02 (m, 3H), 2.76 (brs, 2H), 2.67 (s, 6H), 2.34 (s, 3H), 1.76 (m, 1H), 0.94 (d, 6H), 0.91-0.86 (m, 4H); MS(ESI): 491.3$[M+H]^+$.

N-(4-(4-((cyclohexyl(methyl)amino)methyl)phenyl)-3-(2,4-dihydroxy-5-isopropylphenyl)isoxazol-5-yl)cyclopropanecarboxamide (106). White solid (43.7%): ^{1}H NMR (400MHz, CD_3OD) δ 7.48 (d, *J*=8.3Hz, 2H), 7.35 (d, *J*=8.3Hz, 2H), 6.85 (s, 1H), 6.32 (s, 1H), 4.28 (s, 2H), 3.23 (m, 1H), 3.08 (m, 1H), 2.68 (s, 3H), 2.11 (d, *J*=11.3Hz, 2H), 1.95 (d, *J*=11.3Hz, 2H), 1.80-1.69 (m, 2H), 1.64-1.52 (m, 2H), 1.43-1.31 (m, 2H), 1.30-1.21 (m, 1H), 0.99 (d, 6H), 0.90-0.85 (m, 4H); MS(ESI): 504.3$[M+H]^+$.

N-(3-(2,4-dihydroxy-5-isopropylphenyl)-4-(4-((4-(pyrrolidin-1-yl)piperidin-1-yl)methyl)phenyl)isoxazol-5-yl)cyclopropanecarboxamide (107). White solid (27.5%): ^{1}H NMR (400MHz, CD_3OD) δ 7.37 (d, *J*=8.0Hz, 2H), 7.24 (d, *J*=8.0Hz, 2H), 6.80 (s, 1H), 6.35 (s, 1H), 3.59 (s, 2H), 3.40-3.29 (brs, 4H), 3.16-2.99 (m, 4H), 2.20-2.02 (m, 8H), 1.80-1.68 (m, 3H), 0.93-0.84 (m, 10H); MS(ESI): 545.4$[M+H]^+$.

N-(3-(2,4-dihydroxy-5-isopropylphenyl)-4-(4-((4-morpholinopiperidin-1-yl)methyl)phenyl)isoxazol-5-yl)cyclopropanecarboxamide (108). White solid (30.3%). The hydrochloride salt was

prepared as follows: 400 mg compound **108** was added 25 mL hydrogen chloride solution 4.0 M in dioxane. The solution was stirred for 4h at room temperature before the solvent was removed. The residue was dried in vacuo to give the final product (100%). ^{1}H NMR (400MHz, CD_3OD) δ 7.39 (d, *J*=8.0Hz, 2H), 7.25 (d, *J*=8.0Hz, 2H), 6.80 (s, 1H), 6.32 (s, 1H), 3.69 (t, *J*=4.8Hz, 4H), 3.56 (s, 2H), 3.02 (m, 3H), 2.58 (m, 4H), 2.22 (m, 1H), 2.08 (m, 2H), 1.75 (m, 1H), 1.53 (m, 2H), 0.95-0.84 (m, 10H); ^{13}C NMR (100MHz, d^6-DMSO) δ 172.9, 161.4, 157.3, 156.7, 154.0, 131.3, 131.2, 128.2, 128.0, 127.6, 125.4, 110.1, 106.3, 102.7, 72.3, 71.9, 66.4, 63.2, 62.7, 60.2, 59.6, 58.2, 49.5, 48.4, 25.6, 22.9, 22.6, 13.7, 7.9; MS(ESI): 561.3$[M+H]^+$; HRMS calcd for $C_{32}H_{41}N_4O_5$: 561.3077 (M+H)+ Found: 561.3074.

Acknowledgement

The authors wish to thank Dr. Haiyan Liu for her help in performing the *in vitro* PK study. Grateful thanks for financial support from “Interdisciplinary Cooperation Team” Program for Science and Technology Innovation of the Chinese Academy of Sciences; The National Natural Science Foundation of China (Grant No. 81072580, 81273368 and 21272246); the National Science & Technology Major Project "Key New Drug Creation and Manufacturing Pr ogram" of China (Grant No. 2014ZX09507-002); China Marine Commonweal Research Project (201005022-5); National Science and Technology Major Project of the Ministry of Science and Technology of China(No.2012ZX09301001-007 to MG).

References and Notes

[1] M.E. Feder, G.E. Hofmann, HEAT-SHOCK PROTEINS, MOLECULAR CHAPERONES, AND THE STRESS RESPONSE: Evolutionary and Ecological Physiology, Annu. Rev. Physiol. 61 (1999) 243-282.

[2] D. Picard, Heat-shock protein 90, a chaperone for folding and regulation, Cell. Mol. Life Sci. 59 (2002) 1640-1649.

[3] C. Garrido, S. Gurbuxani, L. Ravagnan, G. Kroemer, Heat Shock Proteins: Endogenous Modulators of Apoptotic Cell Death, Biochem. Biophys. Res. Commun. 286 (2001) 433-442.

[4] L. Neckers, P. Workman, Hsp90 Molecular Chaperone Inhibitors: Are We There Yet? Clin. Cancer Res. 18 (2012) 64-76.

[5] L.H. Pearl, C. Prodromou, Structure and Mechanism of the Hsp90 Molecular Chaperone Machinery, Annu. Rev. Biochem. 75 (2006) 271-294.

[6] A. Maloney, P. Workman, HSP90 as a new therapeutic target for cancer therapy: the story unfolds, Expert Opin. Biol. Ther. 2 (2002) 3-24.

[7] K. Moulick, J.H. Ahn, H. Zong, A. Rodina, L. Cerchietti, E.M. Gomes DaGama, E. Caldas-Lopes, K. Beebe, F. Perna, K. Hatzi, L.P. Vu , X. Zhao, D. Zatorska, T. Taldone, P. Smith-Jones, M. Alpaugh, S.S. Gross, N. Pillarsetty, T. Ku, J.S. Lewis, S.M. Larson, R. Levine, H. Erdjument-Bromage, M.L. Guzman, S.D. Nimer, A. Melnick, L. Neckers, G. Chiosis, Affinity-based proteomics reveal cancer-specific networks coordinated by Hsp90, Nat. Chem. Biol. 7 (2011) 818-826.

[8] V.C. da Silva, C.H. Ramos, The network interaction of the human cytosolic 90 kDa heat shock protein Hsp90: A target for cancer therapeutics, J. Proteomics, 75(2012) 2790-2802.

[9] J. Travers, S. Sharp, P. Workman, HSP90 inhibition: two-pronged exploitation of cancer dependencies, Drug Discov. Today, 17 (2012) 242-252.

[10] G.V. Georgakis, A. Younes, Heat-shock protein 90 inhibitors in cancer therapy:17AAG and beyond, Future Oncol. 1 (2005) 273-281.

[11] M. Hwang, L. Moretti, B. Lu, HSP90 Inhibitors: Multi-Targeted Antitumor Effects and Novel Combinatorial Therapeutic Approaches in Cancer Therapy, Curr. Med. Chem. 6 (2009) 3081-3092.

[12] S.M. Roe, C. Prodromou, R. O'Brien, J.E. Ladbury, P.W. Piper, L.H. Pearl, Structural basis for inhibition of the Hsp90 molecular chaperone by the antitumor antibiotics radiciol and geldanamycin, J. Med. Chem. 42 (1999) 42, 260-266.

[13] I. Hostein, D. Robertson, F. DiStefano, P. Oorkman, P.A. Clarke, Inhibition of signal transduction by 17-allylamino-17-demethoxygeldanamycin results in cytostasis and apoptosis, Cancer Res. 61 (2001) 4003-4009.

[14] J.M. Jez, C.H. Julian, G.R. Chen, M. S. Robert, V. S Daniel, Crystal structure and molecular modeling of 17-DMAG in complex with human Hsp90, Chem. Biol. 10 (2003) 361-368.

[15] M. A. Biamonte, J. Shi, K. Hong, D.C. Hurst, L. Zhang, J. Fan, D.J. Busch, P.L. Karjian, A.A. Maldonado, J.L. Sensintaffar, Y.C. Yang, A. Kamal, R.E. Lough, K. Lundgren, F.J. Burrows, G.A. Timony, T.M. Boehm, S.R Kasibhatla, Orally Active Purine-Based Inhibitors of the Heat Shock

Protein 90, J. Med. Chem. 49 (2006) 817-828.

[16] M. A. Biamonte, R. Van de Water, J.W. Arndt, R.H. Scannevin, D. Perret, W.C. Lee, Heat shock protein 90: Inhibitors in clinical trials. J. Med.Chem. 53 (2010) 3-17.

[17] J. R. Proter, C.C. Fritz, K.M. Depew, Discovery and development of Hsp90 inhibitors: a promising pathway for cancer therapy, Curr. Opin. Chem. Biol. 14 (2010) 412-420.

[18] S. R. Kasibhatla, K. Hong, M.A. Biamonte, D.J. Busch, P.L. Karjian, J.L. Sensintaffar, A. Kamal, R.E. Lough, J. Brekken, K. Lundgren, R. Grecko, G.A. Timony, Y. Ran, R. Mansfield, L.C. Fritz, E. Ulm, F.J. Burrows, M.F. Boehm, Rationally Designed High-Affinity 2-Amino-6-halopurine Heat Shock Protein 90 Inhibitors That Exhibit Potent Antitumor Activity, J. Med.Chem. 50 (2007) 2767-2778.

[19] P. Brough, W. Aherne, X. Barril, J. Borgognoni, K. Boxall, J.E. Cansfield, K.J. Cheung, I.; Collins, N.G.M. Davies, M.J. Drysdale, B. Dymock, S.A. Eccles, H. Finch, A. Fink, A. Hayes, R. Howes, R.E. Hubbard, K. James, A.M. Jordan, A. Lockie, V. Martins, A.; Massey, T.P. Matthews, E. McDonald, C. Northfield, L.H. Pearl, C. Prodromou, S. Ray, F.I. Raynaud, S.D. Roughley, S.Y. Sharp, A. Surgenor, D.L. Walmsley, P. Webb, M. Wodb, P. Workman, L. Wright, 4,5-Diarylisoxazole Hsp90 Chaperone Inhibitors: Potential Therapeutic Agents for the Treatment of Cancer, J. Med. Chem. 51 (2008) 196-218.

[20] H K. Huang, J.M. Veal, R.P. Fadden, J.W. Rice, J. Eaves, J.P. Strachan, A.F. Barabasz, B.E. Foley, T.E. Barta, W. Ma, M.A. Silinski, M. Hu, J.M. Partridge, A. Scott, L.G. DuBois, T. Freed, P.M. Steed, A.J. Ommen, E.D. Smith, P.F. Hughes, A.R. Woodward, G.J. Hanson, W.S. McCall, C.J. Markworth, L. Hinkley, M. Jenks, L. Geng, M. Lewis, J. Otto, B. Pronk, K. Verleysen, S.E. Hall, Discovery of Novel 2-Aminobenzamide Inhibitors of Heat Protein 90 as Potent, Selective and Orally Active Antitumor Agents, J. Med. Chem. 52 (2009) 4288-4305.

[21] P.P. Kung, B. Huang, G. Zhang, J.Z. Zhou, J. Wang, J.A. Digits, J. Skaptason, S. Yamazaki, D. Neul, M. Zientek, J. Elleraas, P. Mehta, M.J. Yin, M.J. Hickey, K.S. Gajiwala, C. Rodgers, J.F.II Davies, M.R. Gehring, Dihydroxyphenylisoindoline Amides as Orally Bioavailable Inhibitors of the Heat Shock Protein 90(HSP90) Molecular Chaperone, J. Med. Chem. 53 (2010) 499-503.

[22] P.P. Kung, L. Funk, J. Meng, M. Collins, J.Z. Zhou, M.C. Johnson, A. Ekker, J. Wang, P. Mehta, M.J. Yin, C. Rodgers, J.F.II Davies, E. Bayman, T. Smeal, K.A. Maegley, M.R. Gehring, Dihydroxylphenyl amides as inhibitors of the Hsp90 molecular chaperone, Bioorg. Med. Chem.

Lett. 18 (2008) 6273-6278.

[23] C.W. Murray, M.G. Carr, O. Callaghan, G. Chessari, M. Congreve, S. Cowan, J.E. Coyle, R. Downham, E. Figueroa, M. Frederickson, B. Graham, R. McMenamin, M.A. O'Brien, S. Patel, T.R. Phillips, G. Williams, A.J. Woodhead, J.A. Woolford, Fragment-Based Drug Discovery Applied to Hsp90.Discovery of Two Lead Series with High Ligand Efficiency, J. Med. Chem. 53 (2010) 5942-5955.

[24] A.J. Woodhead, H. Angove, M.G. Carr, G. Chessari, M. Congreve, J.E. Coyle, J. Cosme, B. Graham, P.J. Day, R. Downham, L. Fazal, R. Feltell, E. Figueroa, M. Frederickson, J. Lewis, R. McMenamin,, C.W. Murray M.A. O'Brien, L. Parra, S. Patel, T. Phillips, D. Rees, S. Rich, D.M. Smith, G. Trewartha, M. Vinkovic, B. Williams, J.A. Woolford, Discovery of (2,4-Dihydroxy-5-isopropylphenyl)-[5-(4-methylpiperazin-1-ylmethyl)-1,3-dihydroisoindol-2-yl] methanone (AT13387), a Novel Inhibitor of the Molecular Chaperone Hsp90 by Fragment Based Drug Design, J. Med. Chem.53 (2010) 5956-5969.

[25] D. A. Proia, R. C. Bates, Ganetespib and HSP90: Translating Preclinical Hypotheses into Clinical Promise, Cancer Res. 74 (2014) 1294-1300.

[26] H-P. Sun, J-M. Jia, F. Jiang, X-L. Xu, F. Liu, X-K. Guo, B. Cherfaoui, H-Z. Huang, Y. Pan, Q-D. You, Identification and optimization of novel Hsp90 inhibitors with tetrahydropyrido[4,3-d]pyrimidines core through shape-based screening, Eur. J. Med. Chem. 79 (2014) 399-412.

[27] E. Tzanetou, S. Liekens, K. M. Kasiotis, G. Melagraki, A. Afantitis, N. Fokialakis, S. A. Haroutounian, Antiproliferative novel isoxazoles: Modeling, virtual screening, synthesis, and bioactivity evaluation, Eur. J. Med. Chem. 81 (2014) 139-149.

[28] E. Casale, N. Amboldi, M. G. Brasca, D. Caronni, N. Colombo, C. Dalvit, E. R. Felder, G. Fogliatto, A. Galvani, A. Isacchi, P. Polucci, L. Riceputi, F. Sola, C. Visco, F. Zuccotto, F. Casuscelli, Fragment-based hit discovery and structure-based optimization of aminotriazoloquinazolines as novel Hsp90 inhibitors, Bioorg. Med. Chem. 22 (2014) 4135-4150.

[29] D. Audisio, D. Methy-Gonnot, C. Radanyi, J-M. Renoir, S. Denis, F. Sauvage, J. Vergnaud-Gauduchon, J-D. Brion, S. Messaoudi, M. Alami, Synthesis and antiproliferative activity of novobiocin analogues as potential hsp90 inhibitors, Eur. J. Med. Chem. 83 (2014) 498-507.

[30] K. Jhaveri, S. O. Ochiana, M. PS Dunphy, J. F. Gerecitano, A. D. Corben, R. I. Peter, Y. Y. Janjigian, E. M. Gomes-DaGama, J. Koren III, S. Modi, G. Chiosis, Heat shock protein 90 inhibitors in the treatment of cancer: current status and future directions, Expert Opin. Investig. Drugs, 23 (2014) 611-628.

[31] J. Ren, J. Li, Y. Wang, W. Chen, A. Shen, H. Liu, D. Chen, D. Cao, Y. Li, N. Zhang, Y. Xu, M. Gneg, J. He, B. Xiong, J. Shen, Identification of a new series of potent diphenol HSP90 inhibitors by fragment merging and structure-based optimization, Bioorg. Med. Chem. Lett. 24 (2014) 2525–2529.

[32] J.F. Cheng, M. Chen, B. Liu, Z. Hou, T. Arrhenius, A. M. Nadzan, Design and synthesis of heterocyclic malonyl-CoA decarboxylase inhibitors, Bioorg. Med. Chem. Lett. 16 (2006) 695-700.

[33] M.P. Bourbeau, J.T. Rider, A convenient synthesis of 4-alkyl-5-aminoisoxazoles, Org. Lett. 8 (2006) 3679-3680.

Figure Captions

Figure 1. Reported HSP90 inhibitors

Figure 2. Binding mode of fragments with HSP90.

Figure 3. Crystal structure of Compound **24** bound to N-terminal HSP90 (PDB ID: 4LWE).

Figure 4. A. Complex of compound **60** with HSP90 (PDB ID: 4LWI); B. Complex of compound **93** with HSP90 (PDB ID: 4LWH).

Figure 5. Western Blotting analysis of the expression of co-chaperone and client proteins of HSP90 after incubation with compounds 93 and 108 in U-87 MG cells.

Figure 6. *In vivo* anti-tumor effect of compound 108 in U-87 MG xenograft model.

Figure 1. Reported HSP90 inhibitors

Figure 2. Binding mode of fragments with HSP90.

Figure 3. Crystal structure of Compound **24** bound to N-terminal HSP90 (PDB ID: 4LWE).

Figure 4. A. Complex of compound **60** with HSP90 (PDB ID: 4LWI); B. Complex of compound **93** with HSP90 (PDB ID: 4LWH).

Figure 5. Western Blotting analysis of the expression of co-chaperone and client proteins of HSP90 after incubation with compounds 93 and 108 in U-87 MG cells.

Figure 6. *In vivo* anti-tumor effect of compound 108 in U-87 MG xenograft model.

Table 1. Binding (FP Assay) and Cell Growth Inhibition (SRB Assay) Data of **23-35**

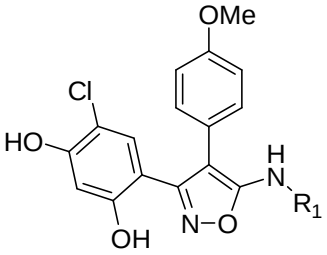

Compound	R_1	FP IC_{50} (μM) [a]	GI_{50} A549 (μM) [a]
23	H	0.053	0.931±0.047
24	MeCO	0.070	7.198±4.810
25	EtCO	0.037	2.364±1.543
26	n-PrCO	0.060	8.487±1.426
27	i-PrCO	0.038	5.533±1.103
28	t-BuCO	0.042	2.301±0.527
29	i-BuCO	0.035	5.976±2.504
30	c-PrCO	0.043	0.761±0.528
31	c-BuCO	0.053	20.687±12.997
32	c-PnCO	0.088	5.476±4.738
33	c-HxCO	0.044	18.728±4.536
34	n-HpCO	0.180	42.877±35.021
35	EtNHCO	0.059	0.926±0.280
NVP-AUY922		0.025	0.026±0.004

[a] Values are reported as the mean of at least two independent determinations.

Table 2. Binding (FP Assay) and Cell Growth Inhibition (SRB Assay) Data of **56-60**

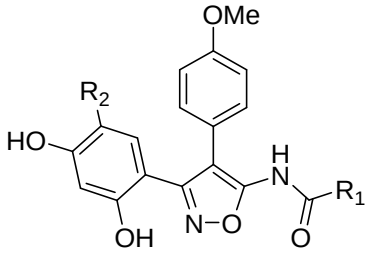

Compound	R_1	R_2	FP IC_{50} (μM) [a]	GI_{50} A549 (μM) [a]
56	Me	Br	0.044	3.764±0.861
57	Me	H	0.140	13.054±4.884
58	Me	Et	0.042	2.099±0.198
59	Me	t-Bu	0.300	6.171±1.047
60	c-Pr	i-Pr	0.023	1.175±0.219

[a] Values are reported as the mean of at least two independent determinations.

Table 3. Binding (FP Assay) and Cell Growth Inhibition (SRB Assay) Data of **93-108**

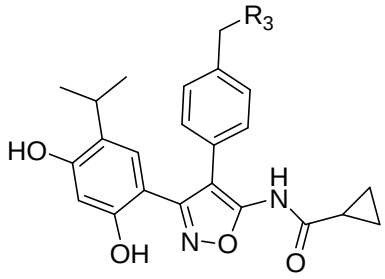

Compound	R_3	FP IC_{50} (μM) [a]	GI_{50} A549 (μM) [a]
93	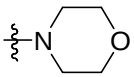	0.027	0.041±0.010
94	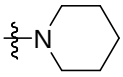	0.017	0.140±0.027
95	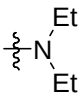	0.021	0.126±0.037
96	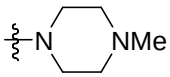	0.027	0.381±0.053
97	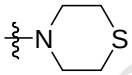	0.057	0.203±0.069
98	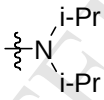	0.035	0.212±0.018
99	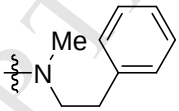	0.14	0.162±0.026
100	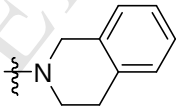	0.036	0.496±0.035
101	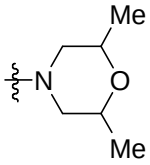	0.029	0.129±0.011
102	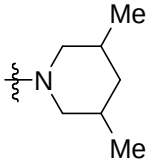	0.046	0.038±0.007

103	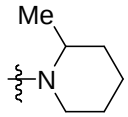	0.035	0.113±0.016
104	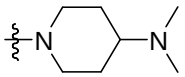	0.070	2.422±0.075
105	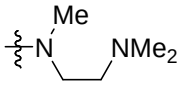	0.055	0.499±0.075
106	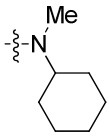	0.058	0.139±0.016
107	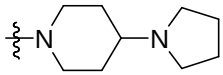	0.044	0.970±0.042
108	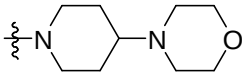	0.030	0.094±0.023

[a] Values are reported as the mean of at least two independent determinations.

Table 4. Cell Growth Inhibition of Compounds **93**, **102** and **108** in Various Human Cancer Cell Lines (μM)

Cell \ Compd	**93**	**102**	**108**
HCC827	0.015±0.002	0.017±0.003	0.035±0.005
NCI-H596	0.166±0.068	0.166±0.056	0.219±0.055
MDA-MB-231	0.054±0.006	0.040±0.004	0.062±0.012
MDA-MB-468	0.042±0.002	0.067±0.015	0.115±0.009
HCC1937	0.114±0.046	0.067±0.001	0.087±0.004
SW620	0.046±0.004	0.035±0.004	0.056±0.008
U-87MG	0.115±0.004	0.111±0.001	0.115±0.013
SW480	0.021±0.007	0.073±0.018	0.082±0.022
HCT116	0.035±0.009	0.025±0.004	0.112±0.011
SMMC-7721	0.046±0.012	0.045±0.006	0.056±0.018
DU-145	0.019±0.001	0.024±0.003	0.045±0.013
OVCAR-8	0.019±0.006	0.027±0.005	0.048±0.006
786-O	0.024±0.005	0.051±0.010	0.069±0.008
Hela	0.046±0.009	0.039±0.008	0.071±0.025
SK-MEL-28	0.090±0.009	0.087±0.023	0.153±0.029

Table 5. HERG safety assay of compounds **93**, **102** and **108**.

Compound	Average % of inhibition at 1 μM concentration
93	10.46±1.78%
102	36.52±0.86%
108	20.83±%4.71
NVP-AUY922	12.92±2.33%

Table 6. Metabolic stability and inhibition of rat and human liver microsomes by compounds **93**, and **108**.

Compound	**93**	**108**	**NVP-AUY922**
RLM Stability Mean Clint(μL/min/mg protein)			
Rat liver Microsome	108	10	180
Human liver Microsome	112	70	92
Direct inhibition Mean(%)			
3A4	NI	9%	12%
2D6	79%	51%	30%
2C9	66%	20%	46%
1A2	22%	23%	23%
TDI(*10^{-4}/min)			
3A4	83	13	38
2D6	22	64	94
2C9	NI	NI	NI
1A2	76	37	8

*NI: No Inhibition

Table 7. Pharmacokinetic profiles of compounds **93** and **108.**

Compound	**93**		**108**	
Administration	p.o.	i.v.	p.o.	i.v.
Dose (mg/kg)	50	10	50	10
Cmax (ng/mL)	438	/	149	/
Tmax (h)	0.083	/	0.25	/
$T_{1/2}$ (h)	1.06	1.62	1.98	6.46
MRT (h)	1.54	1.86	2.71	4.52
AUC_{0-t}(ng·h /mL)	496	615	356	748
F(%)	16.1	/	9.2	/

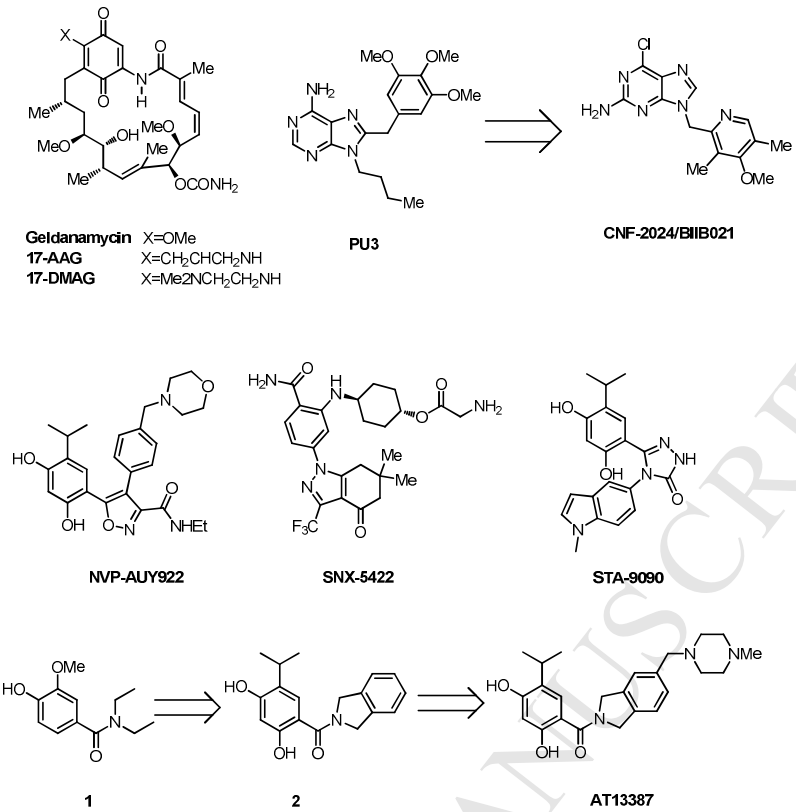

Figure 1. Reported HSP90 inhibitors

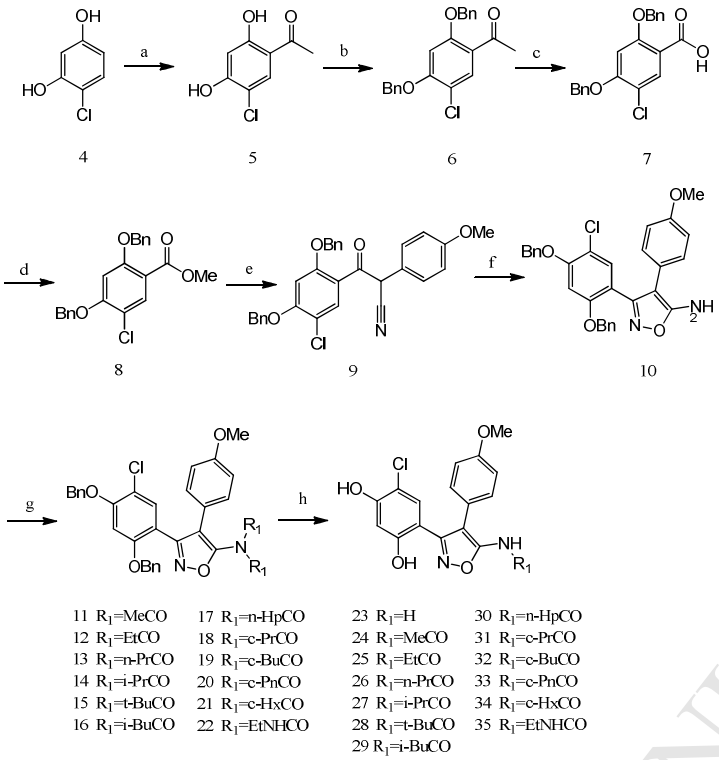

Scheme 1

Reagents and conditions: (a) CH_3COOH, $BF_3 \cdot OEt_2$, 90^oC, 3.5h; (b) $PhCH_2Br$, K_2CO_3, MeCN, 100^oC, 12h; (c) Br_2, NaOH, 1,4-dioxane/H_2O, 12h; (d) CH_3I, K_2CO_3, MeCN, 100^oC, 2h; (e) 4-methoxy phenylacetonitrile, LHMDS, THF, -78 ^oC, 1h; (f) $NH_2OH \cdot HCl$, pyridine, 100^oC, 12h; (g) R_1COCl, NEt_3, DCM, DMAP, 0^oC, 1h, or R_1NCO, NEt_3, DCM, DMAP, 0^oC, 1h; (h) BCl_3, DCM, rt, 1h.

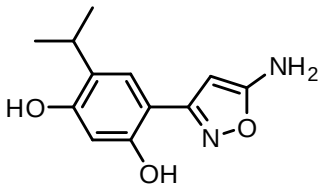

3

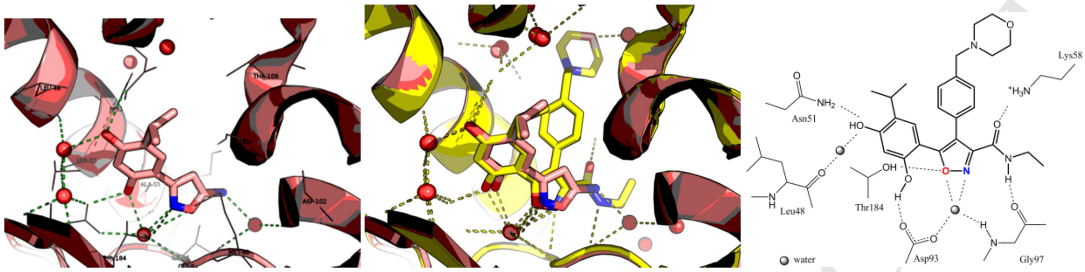

A B C

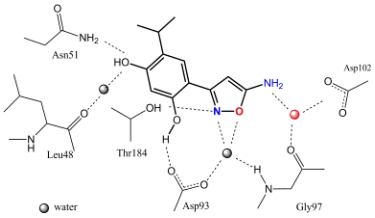

D

Figure 2. Binding mode of fragments with HSP90. (A) Crystal complex of fragment **3** (PDB ID: 4LWF); (B) Overlap of fragment **3** and NVP-AUY922; (C) Binding mode of NVP-AUY922; (D) Binding mode of fragment **3**.

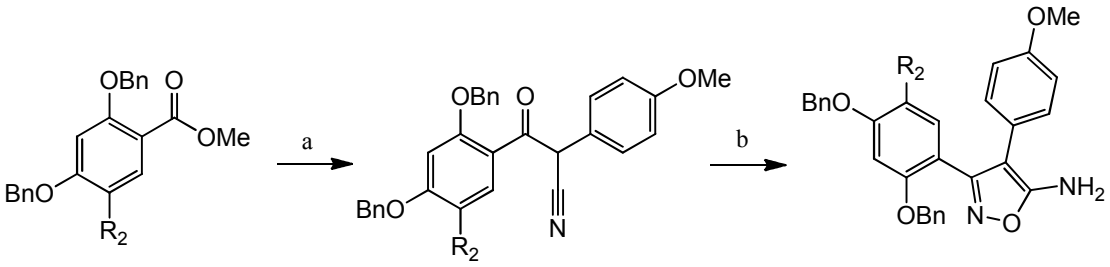

36 R_2=Br
37 R_2=H
38 R_2=Et
39 R_2=i-Pr
40 R_2=t-Bu

41 R_2=Br
42 R_2=H
43 R_2=Et
44 R_2=i-Pr
45 R_2=t-Bu

46 R_2=Br
47 R_2=H
48 R_2=Et
49 R_2=i-Pr
50 R_2=t-Bu

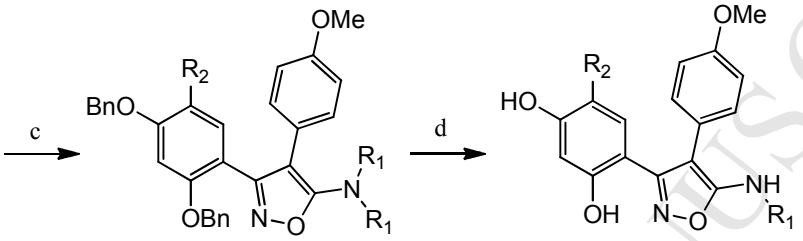

51 R_1=MeCO R_2=Br
52 R_1=MeCO R_2=H
53 R_1=MeCO R_2=Et
54 R_1=MeCO R_2=t-Bu
55 R_1=c-PrCO R_2=i-Pr

56 R_1=MeCO R_2=Br
57 R_1=MeCO R_2=H
58 R_1=MeCO R_2=Et
59 R_1=MeCO R_2=t-Bu
60 R_1=c-PrCO R_2=i-Pr

Scheme 2

Reagents and conditions: (a) 4-methoxy phenylacetonitrile, LHMDS, THF, -78 ^{o}C, 1h; (b) $NH_2OH \cdot HCl$, pyridine, 100^{o}C, 12h; (c) R_1COCl, NEt_3, DCM, DMAP, 0^{o}C, 1h; (d) BCl_3, DCM, rt, 1h.

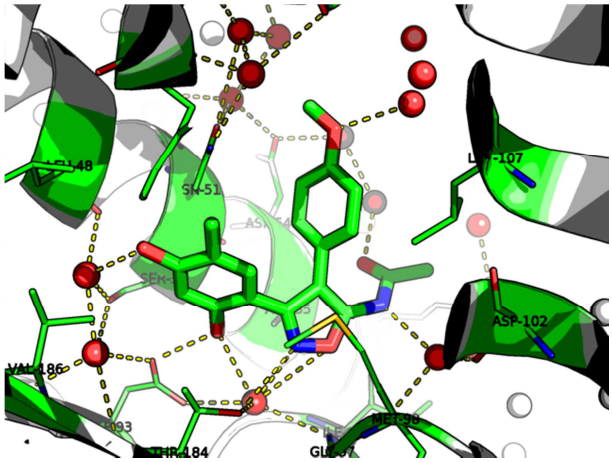

Figure 3. Crystal structure of compound **24** bound to N-terminal HSP90 (PDB ID: 4LWE).

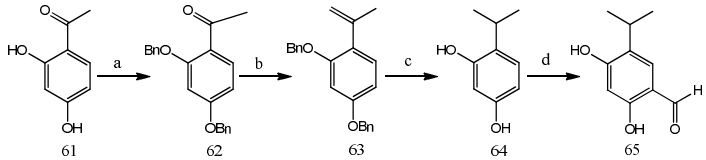

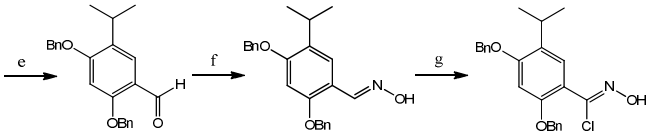

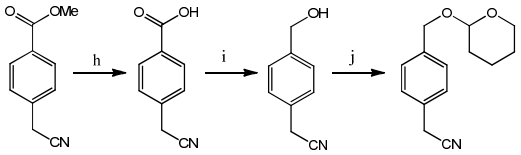

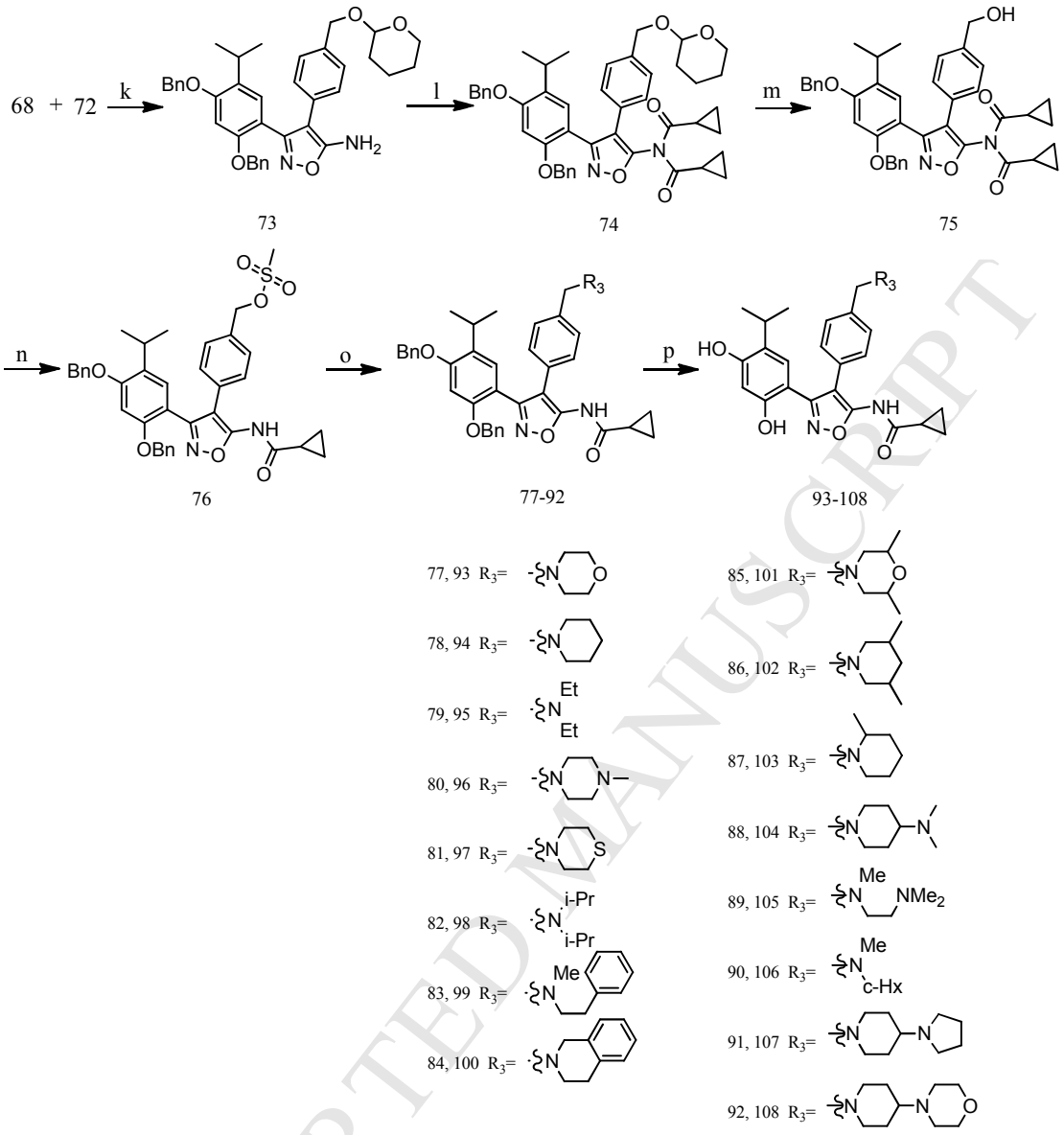

Scheme 3

Reagents and conditions: (a) $PhCH_2Br$, K_2CO_3, MeCN, 100°C, 12h; (b) n-BuLi, $MePPh_3Br$, THF, 0°C, 1h; (c) H_2, Pd/C, EtOH/DCM, 60°C, 12h; (d) $POCl_3$, DMF, 0°C→50°C, 1h; (e) $PhCH_2Br$, K_2CO_3,MeCN, 100°C, 12h; (f) $NH_2OH\cdot HCl$, NaOH, MeOH/H_2O, 80°C, 4h; (g) NCS, DMF, rt, 3h; (h);NaOH, MeOH/H_2O, 80°C, 2h; (i) CDI, THF, rt, 1h then $NaBH_4$, H_2O, rt, 4h; (j) DHP, 4-$MePhSO_3H$, DCM, rt, 0.5h; (k) t-BuLi, THF, -78°C, 1h; (l) c-PrCOCl, NEt_3, DMAP, DCM, rt, 1h; (m) 4-$MePhSO_3H$, MeOH/THF, rt, 0.5h; (n) $MeSO_3Cl$, NEt_3, DCM, rt, 1h; (o) Amines, MeCN, rt, 12h; (p) BCl_3, DCM, rt, 1h.

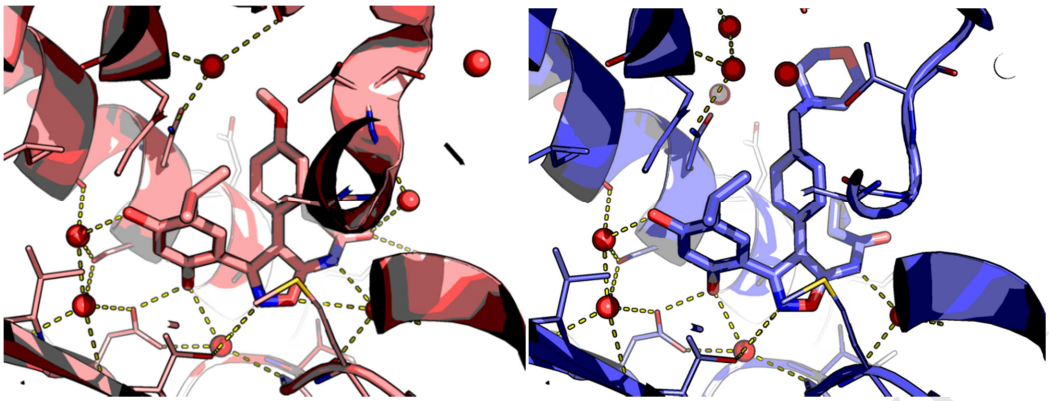

A B

Figure 4. A. Complex of compound **60** with HSP90 (PDB ID: 4LWI); B. Complex of compound **93** with HSP90 (PDB ID: 4LWH).

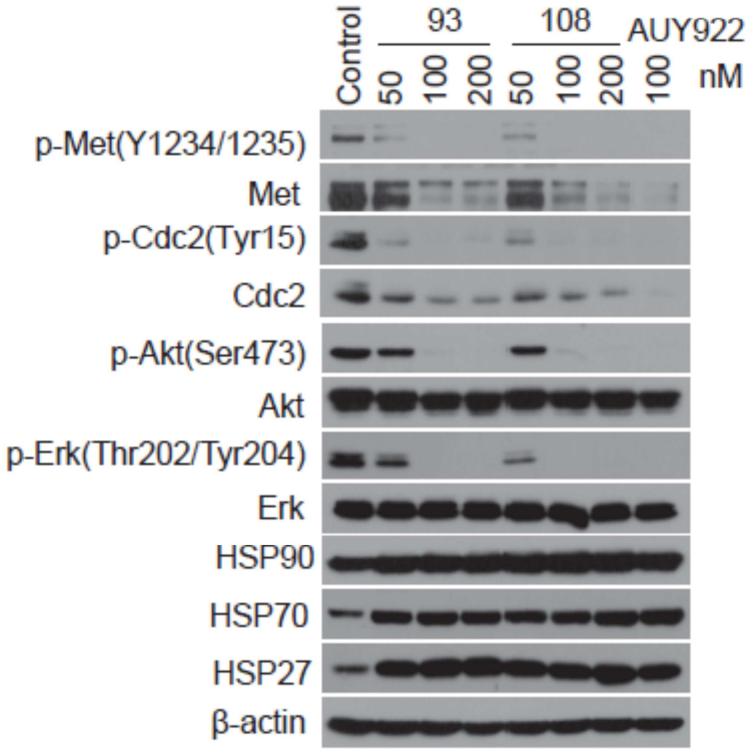

Figure 5. Western Blotting analysis of the expression of co-chaperone and client proteins of HSP90 after incubation with compounds 93 and 108 in U-87 MG cells. U-87 MG cells were incubated with compounds **93** and **108** at indicated concentrations for 24 h. NVP-AUY922 was used as a reference compound. Cell extracts were prepared and subjected to analysis using western blotting with indicated antibodies.

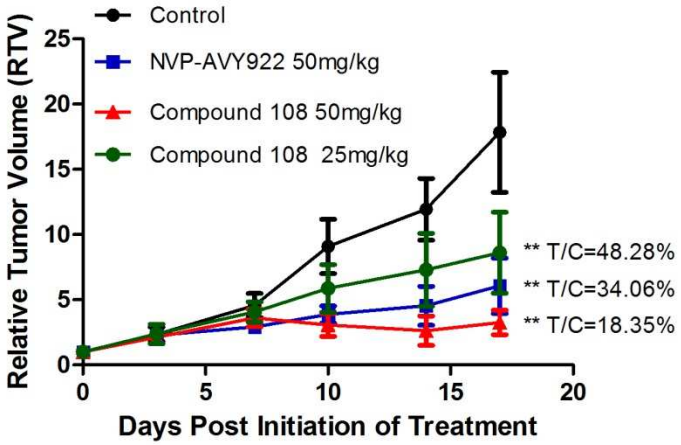

Figure 6. ***In vivo*** **anti-tumor effect of compound 108 in U-87 MG xenograft model.** Compound **108** was administered via intravenous injection 3 times per week for 17 days once the tumor volume reached 100 to 150 mm^3. Tumor volumes were measured twice per week. NVP-AUY922 was used as a reference compound. The value of RTV (relative tumor volume) = V_t/V_0, where V_t is the volume on each day, and V_0 is the volume at the beginning of the treatment. * denotes $p < 0.05$, ** denotes $p < 0.01$, compared to treatment with control, determined with Student's t-test.

- A new scaffold of HSP90 inhibitors was developed with aids of fragment screening and X-ray crystallography techniques.
- Comprehensive assessment was taken.
- Compound **108** exhibited excellent in vivo activities and good pharmacokinetic properties. It is currently advanced to preclinical study.

Supporting Information

Discovery of Potent N-(isoxazol-5-yl)amides as HSP90 Inhibitors

Danqi Chen[1#], Aijun Shen[2#], Jian Li[3#], Feng Shi[1], Wuyan Chen[4], Jing Ren[1], Hongchun Liu[2], Yechun Xu[4*], Xin Wang[1] , Xinying Yang[2], Yiming Sun[2], Min Yang[3], Jianhua He[3], Yueqin Wang[2], Liping Zhang[5], Min Huang[2], Meiyu Geng[2*], Bing Xiong[1*], Jingkang Shen[1*]

[1]*Department of Medicinal Chemistry, State Key Laboratory of Drug Research, Shanghai Institute of Materia Medica, Chinese Academy of Sciences, 555 Zuchongzhi Road, Shanghai 201203, China*

[2]*Division of Anti-tumor Pharmacology, State Key Laboratory of Drug Research, Shanghai Institute of Materia Medica, Chinese Academy of Sciences, 555 Zuchongzhi Road, Shanghai 201203, China*

[3]*Shanghai Institute of Applied Physics, Chinese Academy of Sciences, 239 Zhangheng Road, Shanghai 201204, China*

[4]*Drug Discovery and Design Center, Shanghai Institute of Materia Medica, Chinese Academy of Sciences, 555 Zuchongzhi Road, Shanghai 201203, China*

[5]*Department of Pharmacology and Glycobiology, School of Medicine and Pharmacy, Ocean University of China, 5 Yushan Road, Qingdao 266003, People's Republic of China*

[#]*these authors contributed equally*

* Corresponding authors Tel:86-21-50806600-5412 (B.X) E-mail: bxiong@simm.ac.cn; (Y.X) ycxu@simm.ac.cn; (M.G) mygeng@simm.ac.cn; (J.S)jkshen@simm.ac.cn

^{1}H NMR of Compound 93

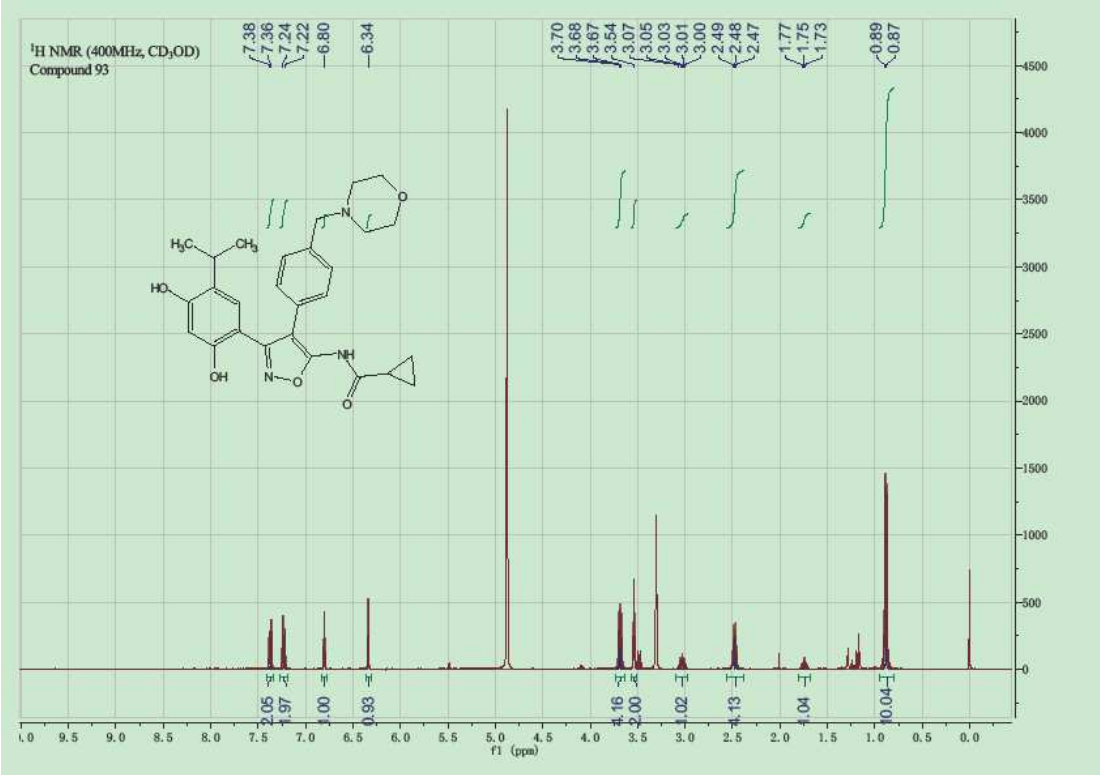

^{13}C NMR of Compound 93

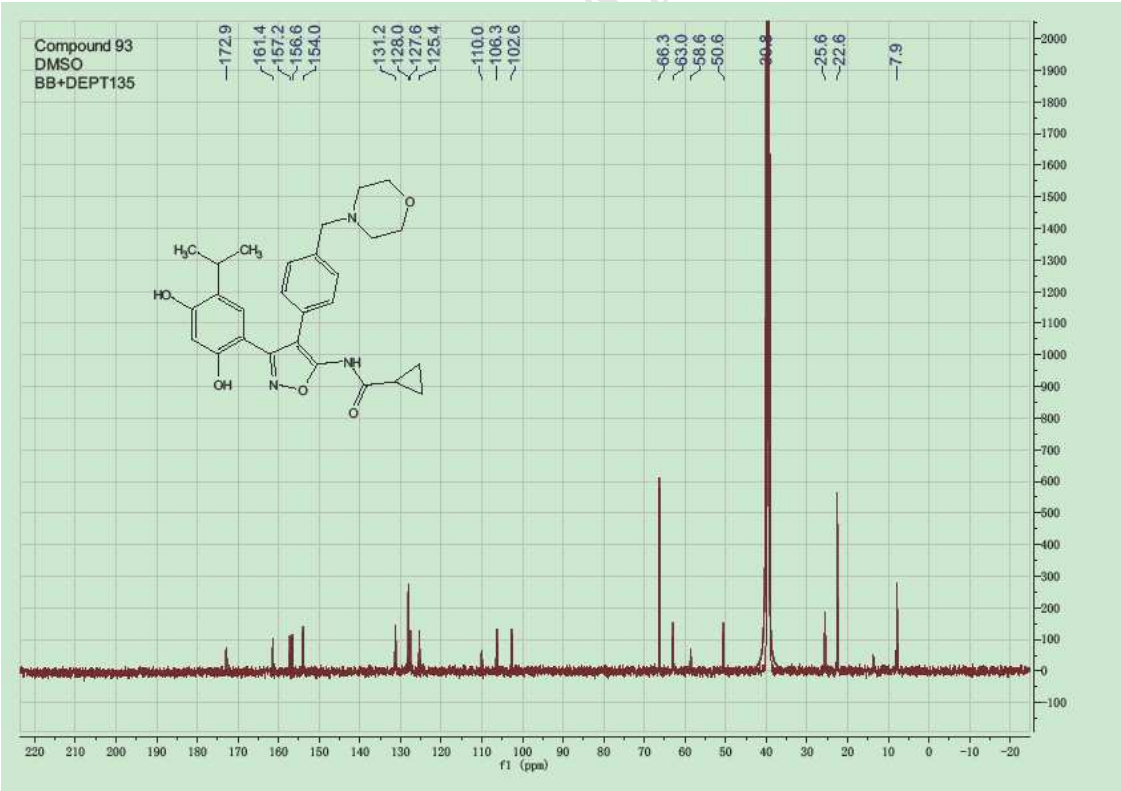

1H NMR of Compound 108

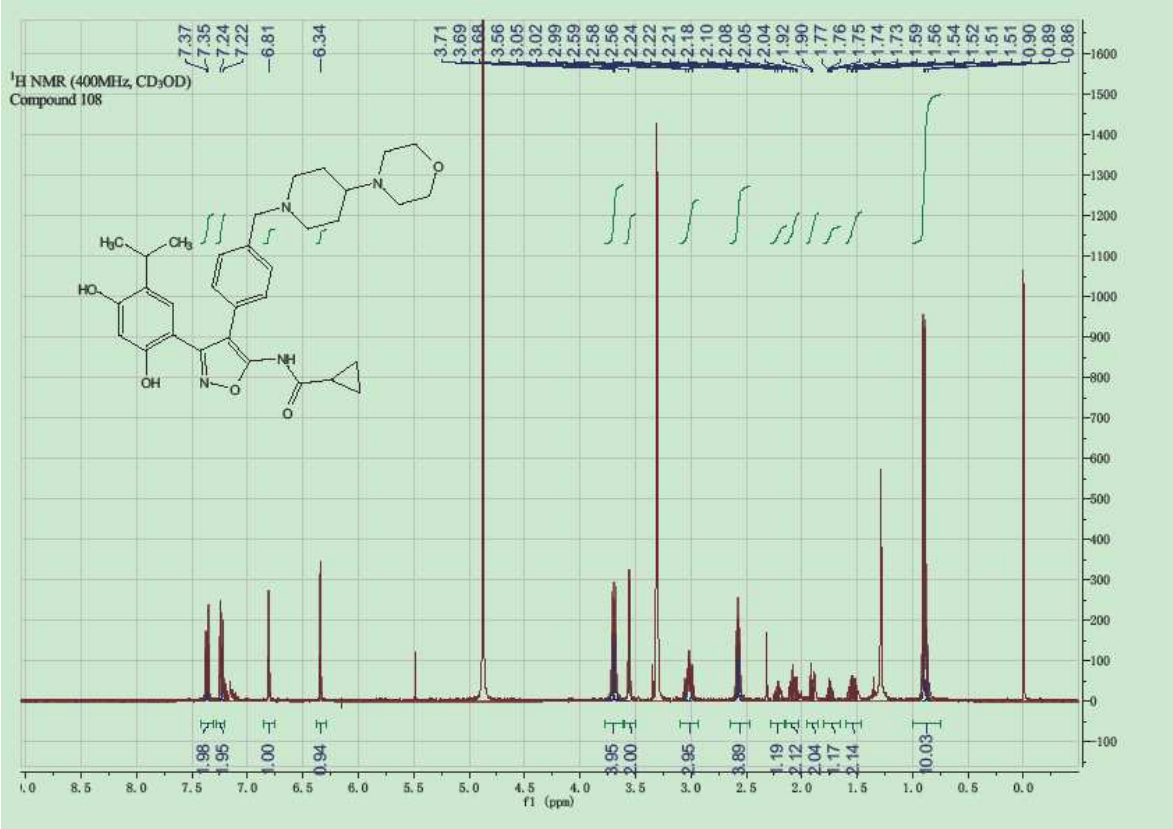

^{13}C NMR of Compound 108